New results in multiboson production from CMS

Giacomo Boldrini [1] - Moriond EW 2025

[1]CNRS/IN2P3 - LLR, École polytechnique

On behalf of the CMS Collaboration

Diboson $Z\gamma$ at CMS

$Z\gamma$ one of the most precisely measurable diboson channels at LHC $\rightarrow$ precise SM tests. Provides unique access to neutral triple gauge couplings as BSM tests.

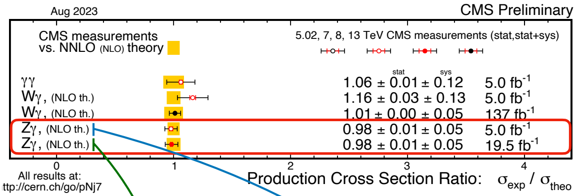

Process	$\sqrt{s}$ TeV	Reference
$Z\gamma \rightarrow \nu\nu\gamma$	13	CMS-PAS-SMP-22-009
$Z\gamma \rightarrow \nu\nu\gamma$	8	Phys.Lett.B760(2016)448
$Z\gamma \rightarrow \ell\ell\gamma$	8	JHEP04(2015)164
$Z\gamma \rightarrow \ell\ell\gamma$	7	Phys.Rev.D89(2014)092005

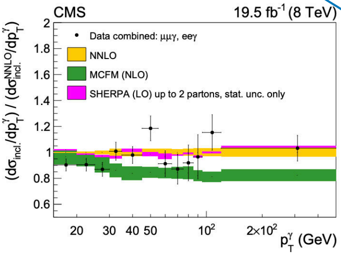

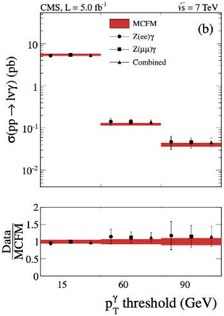

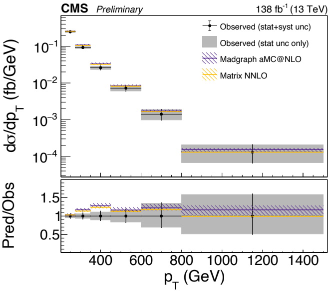

$Z\gamma \to \ell\ell\gamma$ Run 3 - Analysis strategy

New CMS measurement of $Z\gamma \to \ell\ell\gamma$ fiducial cross section at $\sqrt{s} = \mathbf{13.6\ TeV}$. 2022 data with $L = 34.75\ \text{fb}^{-1}$

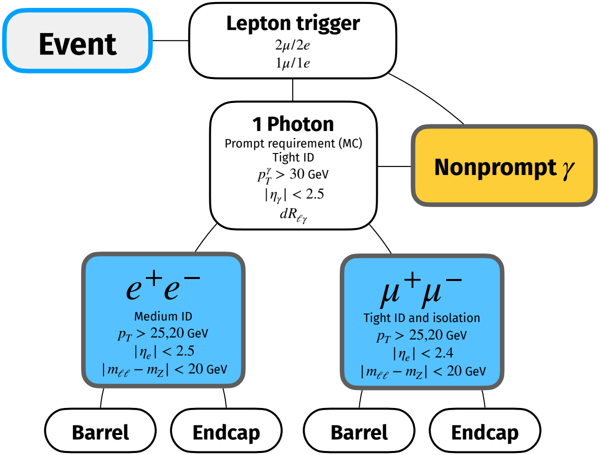

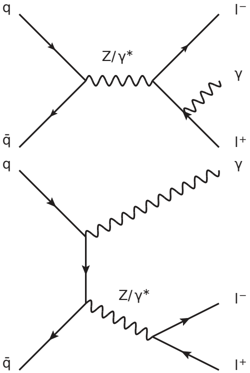

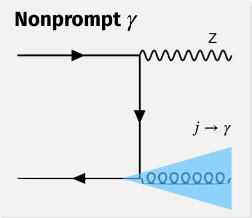

$Z\gamma \to \ell\ell\gamma$ Run 3 - Analysis strategy

Major source of background ($\sim$98%) **nonprompt γ** $\to$ data-driven estimate with **ABCD method** with ECAL shower shape $\sigma_{i\eta i\eta}$ and charged isolation sum I_{ch}:

- **A**: Pass $\sigma_{i\eta i\eta}$, Pass I_{ch}
- **B**: Pass $\sigma_{i\eta i\eta}$, Fail I_{ch}
- **C**: Fail $\sigma_{i\eta i\eta}$, Pass I_{ch}
- **D**: Fail $\sigma_{i\eta i\eta}$, Fail I_{ch}

$$N_A = \left(\frac{N_A \cdot N_D}{N_B \cdot N_C}\right)^{DY} \cdot \left(N_B - N^{\text{prompt}}_{\text{B,sig}} - N^{\text{prompt}}_{\text{B,bkg}}\right) \cdot \left(\frac{N_C - N^{\text{prompt}}_{\text{C,sig}} - N^{\text{prompt}}_{\text{C,bkg}}}{N_D - N^{\text{prompt}}_{\text{D,sig}} - N^{\text{prompt}}_{\text{D,bkg}}}\right)$$

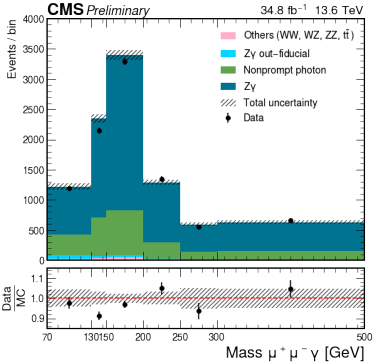

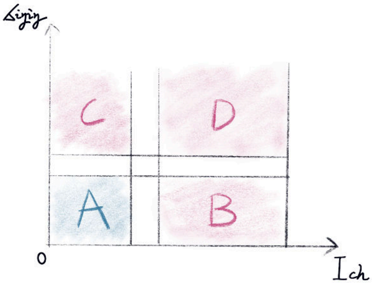

- **Statistical uncertainty**: error propagation of N_A
- **Systematic uncertainty**: change of $(N_A \cdot N_D / N_B \cdot N_C)^{DY}$ with ABCD regions boundaries

Photon ID, luminosity and Nonprompt are the leading uncertainties in the measurement

$Z\gamma \to \ell\ell\gamma$ Run 3 - Results

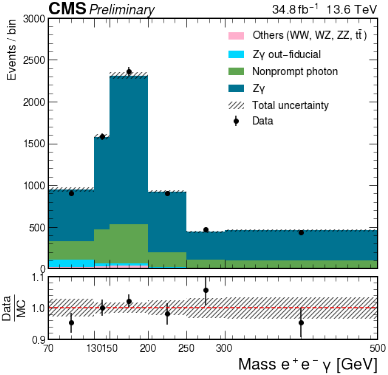

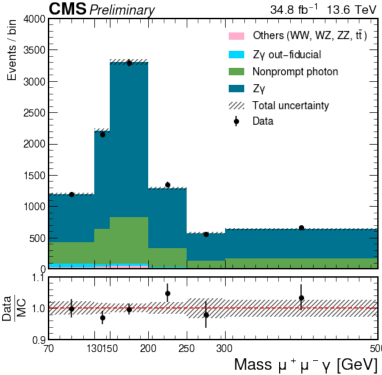

Region	σB $\pm$ theory $\pm$ sys. $\pm$ stat.
$Z\gamma$ ($\mu\mu$) Exp.	0.961 $\pm$ 0.004 $\pm$ 0.028 $\pm$ 0.019
$Z\gamma$ (ee) Exp.	0.961 $\pm$ 0.004 $\pm$ 0.037 $\pm$ 0.021
$Z\gamma$ ($\mu\mu$ + ee) Exp.	1.922 $\pm$ 0.006 $\pm$ 0.056 $\pm$ 0.033
$Z\gamma$ ($\mu\mu$) Obs.	0.928 $\pm$ 0.004 $\pm$ 0.027 $\pm$ 0.018
$Z\gamma$ (ee) Obs.	0.975 $\pm$ 0.003 $\pm$ 0.038 $\pm$ 0.021
$Z\gamma$ ($\mu\mu$ + ee) Obs.	1.896 $\pm$ 0.006 $\pm$ 0.054 $\pm$ 0.033

Good agreement with NLO predictions from MadGraph:

$$\mu_{\text{obs}} = 0.968^{+0.028}_{-0.027}(\text{sys})^{+0.016}_{-0.017}(\text{stat})$$

$$\mu_{\text{exp}} = 1.000^{+0.029}_{-0.027}(\text{sys})^{+0.017}_{-0.017}(\text{stat})$$

Vector Boson Scattering

Vector boson scattering (**VBS**) happens at the LHC when the **two incoming partons radiate electroweak vector bosons that interact** with each other

At LO VBS contributions come from **purely-EW processes** α^6, **QCD-induced** $\alpha_S^2\alpha^4$ and the interference $\alpha_S\alpha^5$

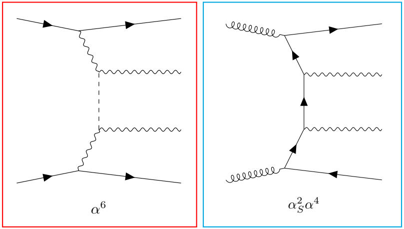

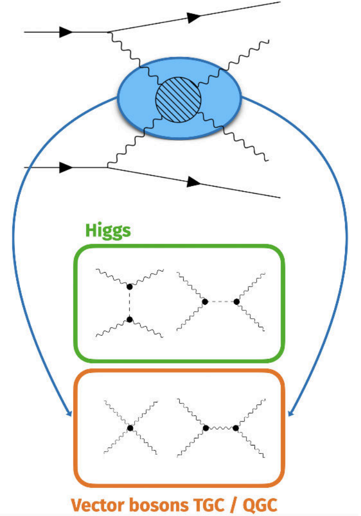

- **Without photons, VBS presents a 6-fermions final state**: 2 jets coming from the initial state partons, 4 coming from the scattered bosons
- **Peculiar kinematical properties:** 2 jets in the forward region with high $\Delta\eta_{jj}$ and m_{jj}.

Vector Boson Scattering in CMS Run II

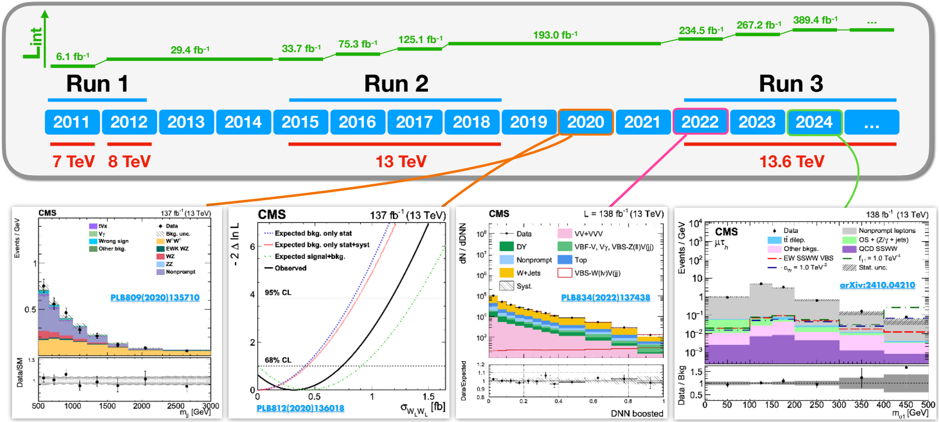

Run II VBS searches refined analyses with clean channels, **multiple observations**. **First time targeting polarized $V_L V_L \to V_L V_L$**. More and more **evidences for complex final states** thanks to 138 fb^{-1}. $\sqrt{s} = 13$ TeV allows for **strongest constraints on aQGC / EFT** parameters.

Input analyses

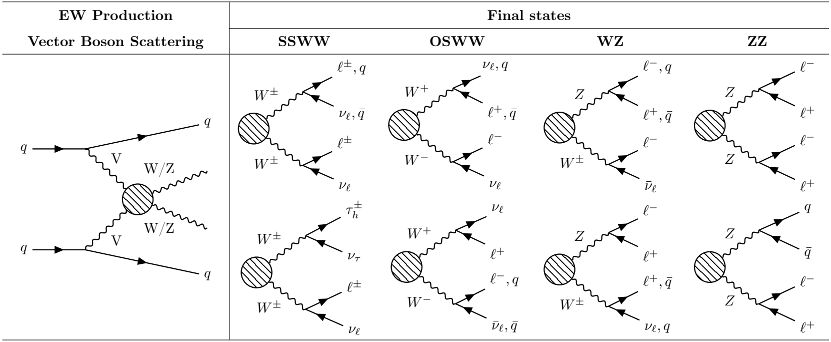

Shorthand name	Production modes	Final state	N. ℓ	Reference
WV	$pp \to W^+W^-jj, W^\pm W^\pm jj, W^\pm Zjj$	$\ell\nu jjjj$	1	[28]
SSWW (e, μ)	$pp \to W^\pm W^\pm jj$	$\ell^\pm\ell^\pm 2\nu jj$	2	[24]
OSWW	$pp \to W^+W^-jj$	$\ell^+\ell^- 2\nu jj$	2	[26]
ZV	$pp \to W^\pm Zjj, ZZjj$	$2\ell jjjj$	2	[29]
SSWW (τ_h)	$pp \to W^\pm W^\pm jj$	$\ell^\pm\tau_h^\pm 2\nu jj$	2	[25]
WZ	$pp \to W^\pm Zjj$	$3\ell\nu jj$	3	[24]
ZZ(4ℓ)	$pp \to ZZjj$	$4\ell jj$	4	[27]

Input analyses

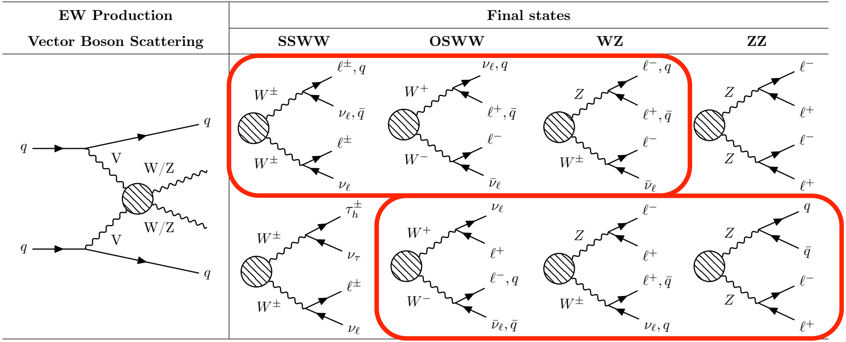

Shorthand name	Production modes	Final state	N. ℓ	Reference
WV	$pp \to W^+W^-jj, W^\pm W^\pm jj, W^\pm Zjj$	$\ell\nu jjjj$	1	[28]
SSWW (e, μ)	$pp \to W^\pm W^\pm jj$	$\ell^\pm\ell^\pm 2\nu jj$	2	[24]
OSWW	$pp \to W^+W^-jj$	$\ell^+\ell^- 2\nu jj$	2	[26]
ZV	$pp \to W^\pm Zjj, ZZjj$	$2\ell jjjj$	2	[29]
SSWW (τ_h)	$pp \to W^\pm W^\pm jj$	$\ell^\pm\tau_h^\pm 2\nu jj$	2	[25]
WZ	$pp \to W^\pm Zjj$	$3\ell\nu jj$	3	[24]
ZZ(4ℓ)	$pp \to ZZjj$	$4\ell jj$	4	[27]

Input analyses

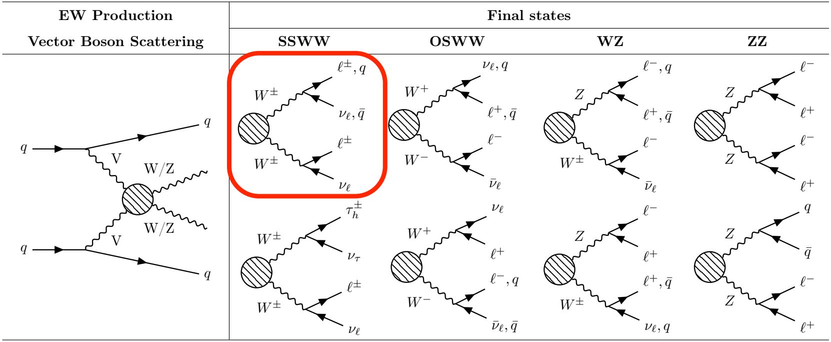

Shorthand name	Production modes	Final state	N. ℓ	Reference
WV	$pp \to W^+W^-jj, W^\pm W^\pm jj, W^\pm Zjj$	$\ell\nu jjjj$	1	[28]
SSWW (e, μ)	$pp \to W^\pm W^\pm jj$	$\ell^\pm\ell^\pm 2\nu jj$	2	[24]
OSWW	$pp \to W^+W^-jj$	$\ell^+\ell^- 2\nu jj$	2	[26]
ZV	$pp \to W^\pm Zjj, ZZjj$	$2\ell jjjj$	2	[29]
SSWW (τ_h)	$pp \to W^\pm W^\pm jj$	$\ell^\pm\tau_h^\pm 2\nu jj$	2	[25]
WZ	$pp \to W^\pm Zjj$	$3\ell\nu jj$	3	[24]
ZZ(4ℓ)	$pp \to ZZjj$	$4\ell jj$	4	[27]

Input analyses

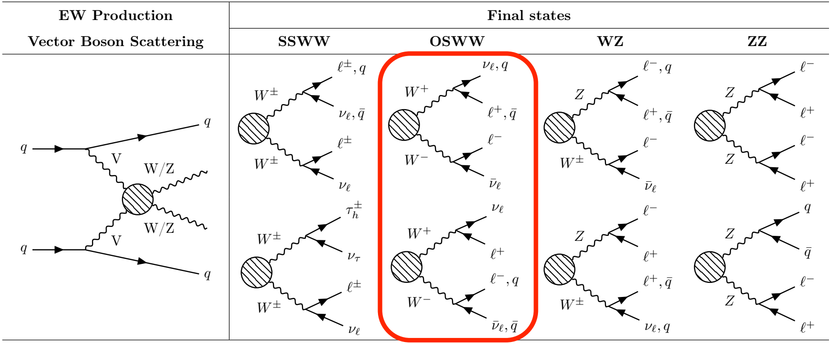

Shorthand name	Production modes	Final state	N. ℓ	Reference
WV	$pp \to W^+W^-jj, W^\pm W^\pm jj, W^\pm Zjj$	$\ell\nu jjjj$	1	[28]
SSWW (e, μ)	$pp \to W^\pm W^\pm jj$	$\ell^\pm\ell^\pm 2\nu jj$	2	[24]
OSWW	$pp \to W^+W^-jj$	$\ell^+\ell^- 2\nu jj$	2	[26]
ZV	$pp \to W^\pm Zjj, ZZjj$	$2\ell jjjj$	2	[29]
SSWW (τ_h)	$pp \to W^\pm W^\pm jj$	$\ell^\pm\tau_h^\pm 2\nu jj$	2	[25]
WZ	$pp \to W^\pm Zjj$	$3\ell\nu jj$	3	[24]
ZZ(4ℓ)	$pp \to ZZjj$	$4\ell jj$	4	[27]

Input analyses

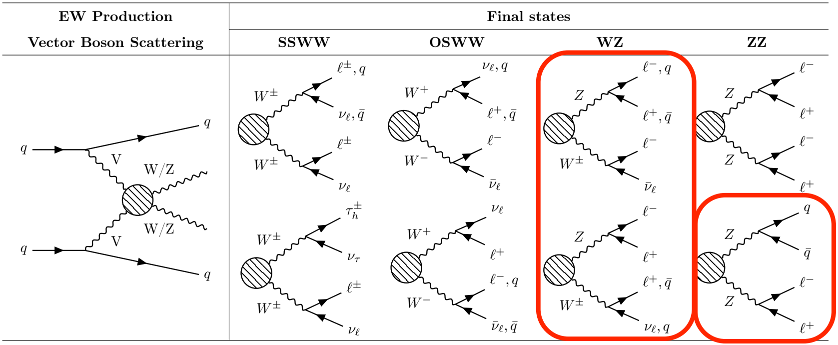

Shorthand name	Production modes	Final state	N. ℓ	Reference
WV	$pp \rightarrow W^+W^-jj, W^\pm W^\pm jj, W^\pm Zjj$	$\ell\nu jjjj$	1	[28]
SSWW (e, μ)	$pp \rightarrow W^\pm W^\pm jj$	$\ell^\pm\ell^\pm 2\nu jj$	2	[24]
OSWW	$pp \rightarrow W^+W^-jj$	$\ell^+\ell^- 2\nu jj$	2	[26]
ZV	$pp \rightarrow W^\pm Zjj, ZZjj$	$2\ell jjjj$	2	[29]
SSWW (τ_h)	$pp \rightarrow W^\pm W^\pm jj$	$\ell^\pm\tau_h^\pm 2\nu jj$	2	[25]
WZ	$pp \rightarrow W^\pm Zjj$	$3\ell\nu jj$	3	[24]
ZZ(4ℓ)	$pp \rightarrow ZZjj$	$4\ell jj$	4	[27]

Input analyses

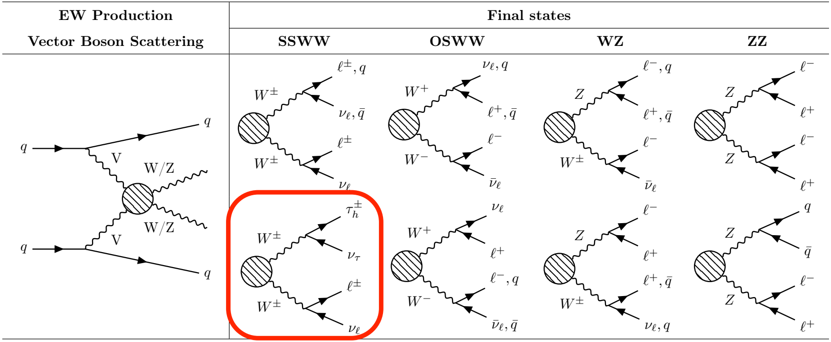

Shorthand name	Production modes	Final state	N. ℓ	Reference
WV	$pp \to W^+W^-jj, W^\pm W^\pm jj, W^\pm Zjj$	$\ell\nu jjjj$	1	[28]
SSWW (e, μ)	$pp \to W^\pm W^\pm jj$	$\ell^\pm\ell^\pm 2\nu jj$	2	[24]
OSWW	$pp \to W^+W^-jj$	$\ell^+\ell^- 2\nu jj$	2	[26]
ZV	$pp \to W^\pm Zjj, ZZjj$	$2\ell jjjj$	2	[29]
SSWW (τ_h)	$pp \to W^\pm W^\pm jj$	$\ell^\pm\tau_h^\pm 2\nu jj$	2	[25]
WZ	$pp \to W^\pm Zjj$	$3\ell\nu jj$	3	[24]
ZZ(4ℓ)	$pp \to ZZjj$	$4\ell jj$	4	[27]

Input analyses

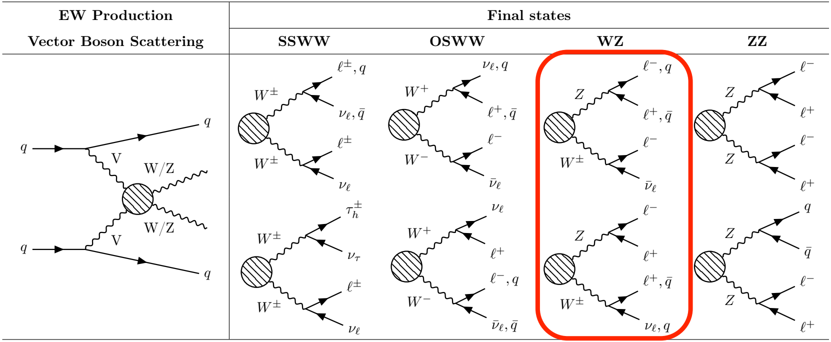

Shorthand name	Production modes	Final state	N. ℓ	Reference
WV	$pp \to W^+W^-jj, W^\pm W^\pm jj, W^\pm Zjj$	$\ell\nu jjjj$	1	[28]
SSWW (e, μ)	$pp \to W^\pm W^\pm jj$	$\ell^\pm\ell^\pm 2\nu jj$	2	[24]
OSWW	$pp \to W^+W^-jj$	$\ell^+\ell^- 2\nu jj$	2	[26]
ZV	$pp \to W^\pm Zjj, ZZjj$	$2\ell jjjj$	2	[29]
SSWW (τ_h)	$pp \to W^\pm W^\pm jj$	$\ell^\pm\tau_h^\pm 2\nu jj$	2	[25]
WZ	$pp \to W^\pm Zjj$	$3\ell\nu jj$	3	[24]
ZZ(4ℓ)	$pp \to ZZjj$	$4\ell jj$	4	[27]

Input analyses

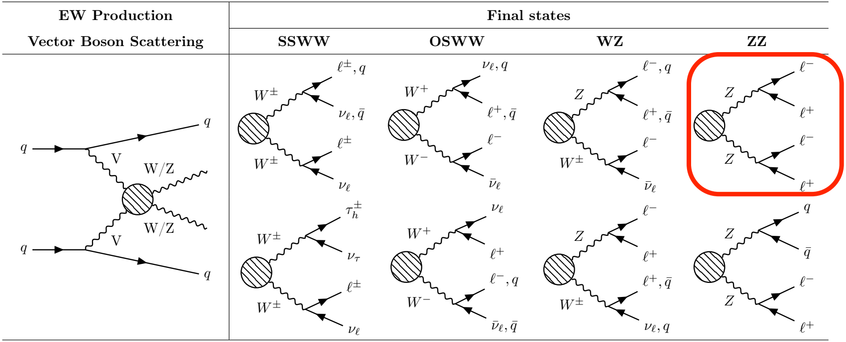

Shorthand name	Production modes	Final state	N. ℓ	Reference
WV	$pp \to W^+W^-jj, W^\pm W^\pm jj, W^\pm Zjj$	$\ell\nu jjjj$	1	[28]
SSWW (e, μ)	$pp \to W^\pm W^\pm jj$	$\ell^\pm\ell^\pm 2\nu jj$	2	[24]
OSWW	$pp \to W^+W^-jj$	$\ell^+\ell^- 2\nu jj$	2	[26]
ZV	$pp \to W^\pm Zjj, ZZjj$	$2\ell jjjj$	2	[29]
SSWW (τ_h)	$pp \to W^\pm W^\pm jj$	$\ell^\pm\tau_h^\pm 2\nu jj$	2	[25]
WZ	$pp \to W^\pm Zjj$	$3\ell\nu jj$	3	[24]
ZZ(4ℓ)	$pp \to ZZjj$	$4\ell jj$	4	[27]

Two combination models: one with four parameters of interest (4-POIs) and the other with six parameters of interest (6-POIs). The former provides a **global investigation of VBS** processes. The latter extends the analysis by **probing the expected production charge asymmetry**

6 parameters	4 parameters
$W^{\pm}W^{\mp}$, $W^{+}W^{+}$, $W^{-}W^{-}$, $W^{+}Z$, $W^{-}Z$, ZZ	$W^{\pm}W^{\pm}$, $W^{\pm}W^{\mp}$, $W^{\pm}Z$, ZZ

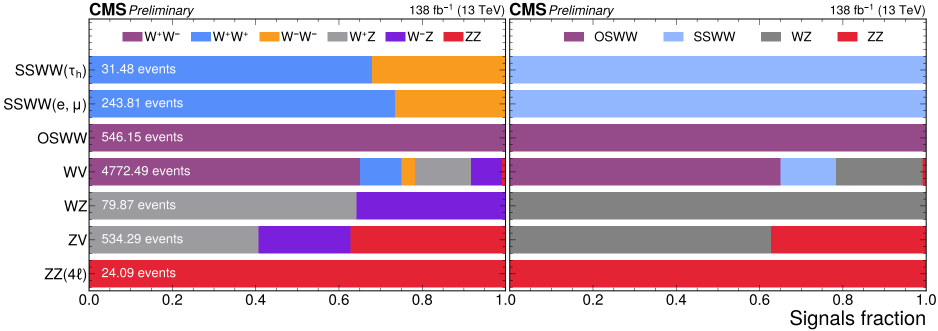

Results

		OSWW	SSWW		WZ		ZZ
4-POI	μ	$1.09^{+0.21}_{-0.18}$ $\left(^{+0.20}_{-0.19}\right)$	$1.04^{-0.14}_{-0.14}$ $\left(^{+0.14}_{-0.14}\right)$		$1.19^{+0.28}_{-0.23}$ $\left(^{+0.29}_{-0.24}\right)$		$1.15^{+0.44}_{-0.37}$ $\left(^{+0.44}_{-0.37}\right)$
	σ	6.2 (6.1)	$\gg 5$ ($\gg 5$)		7.0 (5.5)		4.0 (3.6)
6-POI		W^+W^-	W^+W^+	W^-W^-	W^+Z	W^-Z	ZZ
	μ	$1.08^{+0.20}_{-0.19}$ $\left(^{+0.18}_{-0.18}\right)$	$1.11^{+0.17}_{-0.15}$ $\left(^{+0.14}_{-0.16}\right)$	$0.84^{+0.27}_{-0.24}$ $\left(^{+0.28}_{-0.25}\right)$	$1.15^{+0.32}_{-0.27}$ $\left(^{+0.32}_{-0.27}\right)$	$1.30^{+0.47}_{-0.40}$ $\left(^{+0.44}_{-0.37}\right)$	$1.16^{+0.44}_{-0.38}$ $\left(^{+0.42}_{-0.35}\right)$
	σ	6.1 (6.1)	$\gg 5$ ($\gg 5$)	4.0 (4.6)	5.7 (4.7)	4.2 (3.2)	4.0 (3.6)

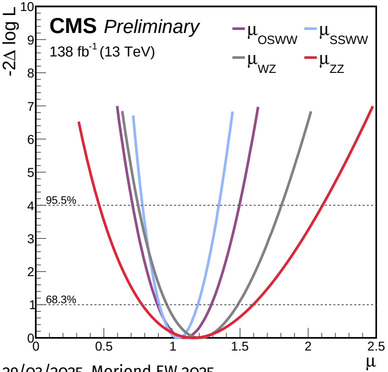

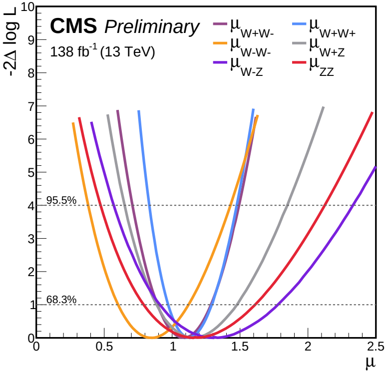

Results

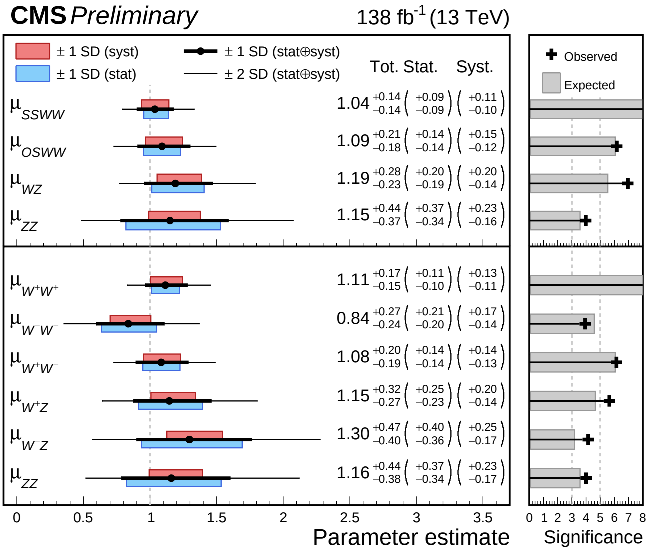

5-10% improvement on signal strengths. Evidence for all charged parameters

S/B plots

Prefit log(S/B) plots show good agreement with SM predictions at LO differentially

- For all bins of the input templates, prefit $\log[S(\mu = 1)/B]$ is computed
- Postfit yields of signal, backgrounds and data is assigned to the leading signal distribution, in terms of yield $\rightarrow$ data is not shown twice.
- Uncertainty on background prediction computed with 500 toys

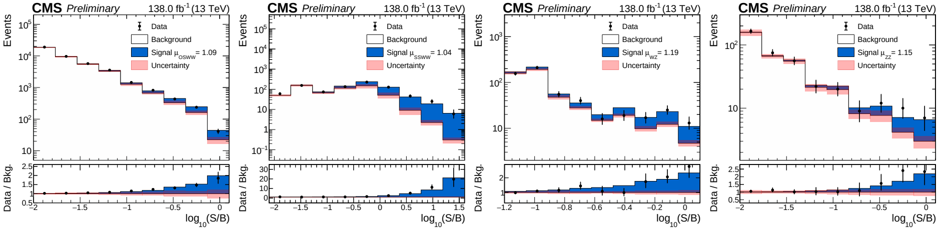

Conclusions

New cross section measurement at $\sqrt{s} = 13.6$ for $Z\gamma \to \ell\ell\gamma$

- **Completes previous measurements at 7,8,13 TeV**
- Attention to **nonprompt** γ estimate: leading background and uncertainty
- **Fiducial cross-sections in agreement with SM@NLO, per-cent level uncertainties**

The SM VBS combination is a first step towards a global interpretation of the VBS processes: polarization, EFT, ...

- 7 channels combined (5 leptonic, 2 semileptonic). **Good agreement with SM**
- **5-10% improvement** on μ measurement. **Evidence for all 6 charged parameters**

BACKUP

VBS is a fundamental probe to understand the electroweak symmetry breaking mechanism

The presence of the Higgs field regularizes the VBS cross-section by canceling exactly the E^2 behaviour of bosonic-only processes.

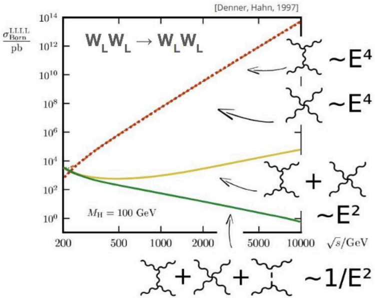

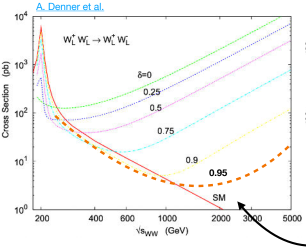

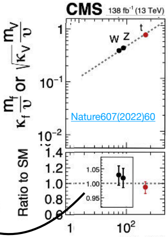

~5% Uncertainty on hVV couplings

A delicate equilibrium: if Higgs boson not SM one (δ), energy-growth of $V_L V_L \rightarrow V_L V_L$ cross section $\rightarrow$ **New physics**

Leptonic VBS $ZZ \to 4l$

Final state with **2 VBS-jets and two pairs of oppositely charged isolated leptons** with same flavour compatible with decay products of a Z boson.

PhysLettB812(2021)135992

Region	EW-VBS	QCD-ZZ	Irr.	Z+jets
Inclusive	6.5%	82.3%	8.7%	2.5%
Loose	21.0%	71.7%	5.3%	2.1%
Tight	48.4%	46.2%	3.7%	1.7%

Regions

- EW significance, total fiducial cross sections and search for aQGCs in ZZ**-inclusive region** $m_{jj} > 100$ GeV
- fiducial cross section measurements done in **two VBS-enriched** regions with $\Delta\eta > 2.4$ and $m_{jj} > 400$ GeV or $m_{jj} > 1$ TeV
- **One background control region** with events from inclusive region not entering the loose VBS-enriched region

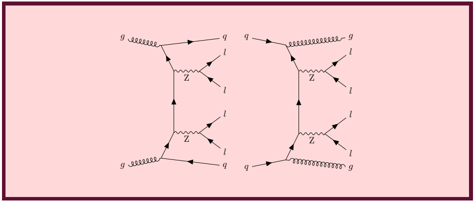

Backgrounds

- Dominant QCD-induced ZZ production ($q\bar{q} \to ZZ$, $gg \to ZZ$)
- $t\bar{t}Z$+jets, VVZ+jets irreducible
- Fake and non-prompt leptons mainly from Z+jets but also $t\bar{t}$+jets, WZ+jets

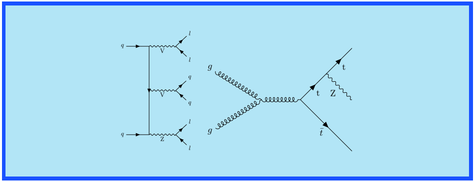

Leptonic VBS ZZ $\to 4l$

Signal extracted with Matrix Element Discriminant (K_D). Check that MVAs bring no significant gain

- **Evidence for EW VBS production** 4.0 σ (3.5 expected)
- Cross section (EW and EW+QCD) measured in three fiducial volumes with VBS-EW simulation at LO and NLO **Good agreement with SM**

Region	σ (EW) fb
Inclusive	$0.33^{+0.11}_{-0.10}$(stat)$^{+0.04}_{-0.03}$(syst)
Loose	$0.180^{+0.070}_{-0.060}$(stat)$^{+0.021}_{-0.012}$(syst)
Tight	$0.09^{+0.04}_{-0.03}$(stat) $\pm$ 0.02(syst)

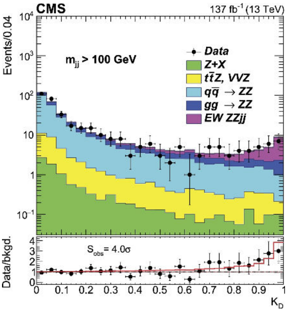

Limits on Wilson coefficients (W.c.) of transverse (T) dimension-8 operators extracted from m_{4l} distribution. The VBS-ZZ is extremely sensitive to charged (T_0, T_1, T_2) and neutral operators (T_8, T_9)

- **Unitarization** of the scattering amplitude $|\mathcal{A}_{SM} + \frac{f_i}{\Lambda^4}\mathcal{A}_{\mathcal{O}_8}|$ taken into account
- **No significant deviations from SM observed**

Coupling	Exp. lower	Exp. upper	Obs. lower	Obs. upper	Unitarity bound
f_{T0}/Λ^4	−0.37	0.35	−0.24 (−0.26)	0.22 (0.24)	2.4
f_{T1}/Λ^4	−0.49	0.49	−0.31 (−0.34)	0.31 (0.34)	2.6
f_{T2}/Λ^4	−0.98	0.95	−0.63 (−0.69)	0.59 (0.65)	2.5
f_{T8}/Λ^4	−0.68	0.68	−0.43 (−0.47)	0.43 (0.48)	1.8
f_{T9}/Λ^4	−1.5	1.5	−0.92 (−1.02)	0.92 (1.02)	1.8

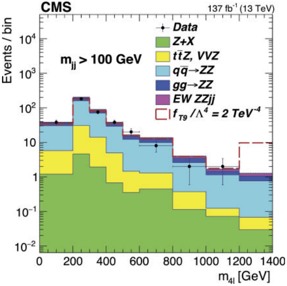

Leptonic VBS $W^{\pm}W^{\pm} \to 2l^{\pm}2\nu$

Final state with **2 VBS-jets, two isolated leptons with same charge and MET**. A Significant background comes from VBS-WZ $\to$ **measure** $W^{\pm}W^{\pm}$ **and** WZ **together**

Golden channel: the presence of two same-signed leptons reduces drastically the QCD-induced background

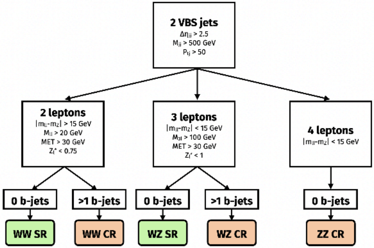

Backgrounds

- **Dominant non-prompt**, estimated from data
- **Wrong-sign** from mischarge identification mainly from Z+jets
- **EW VBS** $W^{\pm}Z$ where one Z-lepton is lost
- **QCD-induced** $W^{\pm}W^{\pm}$ + 2jets and $W^{\pm}Z$ + 2jets
- QCD and EW induced **ZZ + 2jets**

The Zeppenfeld variable Z_l used to reduce QCD-induced background $Z_X = |\eta_X - \bar{\eta}_j|/|\Delta\eta_{jj}|$. Plot from P. Govoni, C. Mariotti

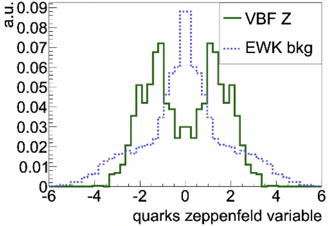

Maximum Likelihood (ML) fit to 5 regions simultaneously. **Including NLO EW+QCD corrections** ($\mathcal{O}$(10%)) at order α^7, $\alpha_S\alpha^6$ to VBS $W^{\pm}W^{\pm}$ and WZ

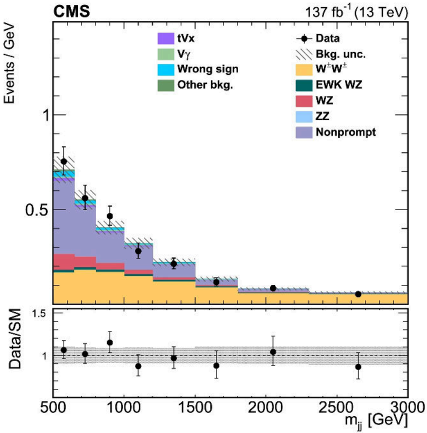

Observables

- $W^{\pm}W^{\pm}$ signal extracted with **2D variable**: $\mathbf{m_{ll}}$ and $\mathbf{m_{jj}}$
- **Boosted Decision Tree** trained for EW VBS WZ
- $\mathbf{m_{jj}}$ to measure WZ-QCD and ZZ normalization from data

The VBS EW production of $W^{\pm}W^{\pm}$ is observed with a significance » 5σ

Leptonic VBS $W^{\pm}Z \rightarrow 3l\nu$

The VBS production of WZ is treated as a background to the $W^{\pm}W^{\pm}$ analysis but **is an interesting process by itself**. Measured together with $W^{\pm}W^{\pm}$.

Backgrounds

- **Dominant QCD induced**
- **Non-prompt** estimated from data
- **Wrong-sign** from mischarge identification mainly from Z+jets
- QCD and EW induced **ZZ + 2jets**

In order to reduce the overwhelming QCD background **a BDT is employed to extract the signal** trained with reported variables

Variable	Definition
m_{jj}	Mass of the leading and trailing jets system
$\Delta\eta_{jj}$	Absolute difference in rapidity of the leading and trailing jets
$\Delta\phi_{jj}$	Difference in azimuth angles of the leading and trailing jets
p_T^{j1}	p_T of the leading jet
p_T^{j2}	p_T of the trailing jet
η^{j1}	Pseudorapidity of the leading jet
$\|\eta^W - \eta^Z\|$	Absolute difference between the rapidities of the Z boson and the lepton from the decay of the W boson
$z^*_{\ell_i} (i = 1,2,3)$	Zeppenfeld variable of the three selected leptons: $z^*_\ell = \|\eta_{\ell_i} - (\eta_{j1} + \eta_{j2})/2.\|/\Delta\eta_{jj}$
$z^*_{3\ell}$	Zeppenfeld variable of the triple-lepton system
$\Delta R_{j1,Z}$	The ΔR between the leading jet and the Z boson
$\|\vec{p}_T^{tot}\|/\sum_i p_T^i$	Transverse component of the vector sum of the bosons and tagging jets momenta, normalised to their scalar p_T sum

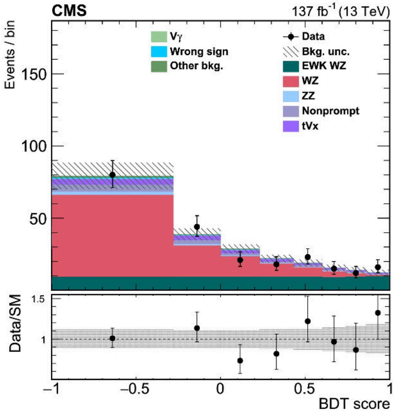

The VBS EW production of $W^{\pm}Z$ is observed with a significance of 6.8σ (5.3 expected)

Inclusive and differential cross-sections measurements are reported in fiducial phase spaces for $W^{\pm}W^{\pm}$ and $W^{\pm}Z$ with selections targeting VBS-signature. **Good agreement with SM**

Process	$\sigma\mathcal{B}$ (fb)	Theory prediction (fb)	Theory prediction with NLO corrections (fb)
EW $W^{\pm}W^{\pm}$	3.98 ± 0.45 $(0.37\ (\text{stat}) \pm 0.25\ (\text{syst}))$	3.93 ± 0.57	3.31 ± 0.47
EW+QCD $W^{\pm}W^{\pm}$	4.42 ± 0.47 $(0.39\ (\text{stat}) \pm 0.25\ (\text{syst}))$	4.34 ± 0.69	3.72 ± 0.59
EW WZ	1.81 ± 0.41 $(0.39\ (\text{stat}) \pm 0.14\ (\text{syst}))$	1.41 ± 0.21	1.24 ± 0.18
EW+QCD WZ	4.97 ± 0.46 $(0.40\ (\text{stat}) \pm 0.23\ (\text{syst}))$	4.54 ± 0.90	4.36 ± 0.88
QCD WZ	3.15 ± 0.4 $(0.45\ (\text{stat}) \pm 0.18\ (\text{syst}))$	3.12 ± 0.70	3.12 ± 0.70

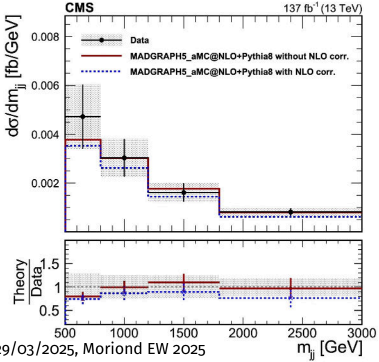

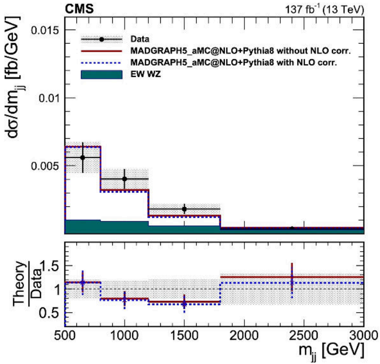

Anomalous quartic gauge coupling search carried under **EFT** framework constraining dimension-8 operators.
Cannot define m_{VV}, 2D variable with **transverse mass m_T and m_{jj}**

- **9 operators** investigated
- No unitarization procedure is applied → **Clipping EFT predictions at limit**
- **No excess of events with respect to the SM is observed**

$$m_T(VV) = \sqrt{(\sum_i E_i)^2 - \sum_i p_{z,i})^2}$$

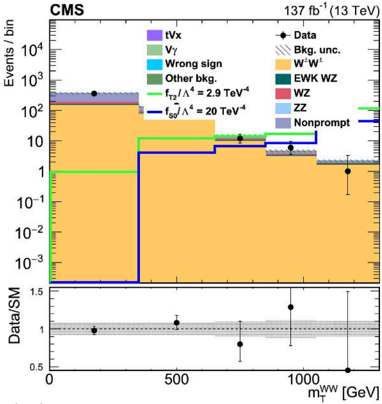

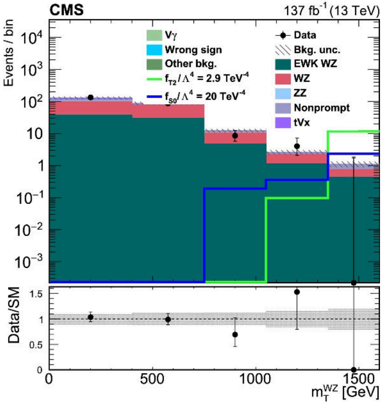

Leptonic $W^\pm W^\pm \to 2\ell 2\nu$ CMS

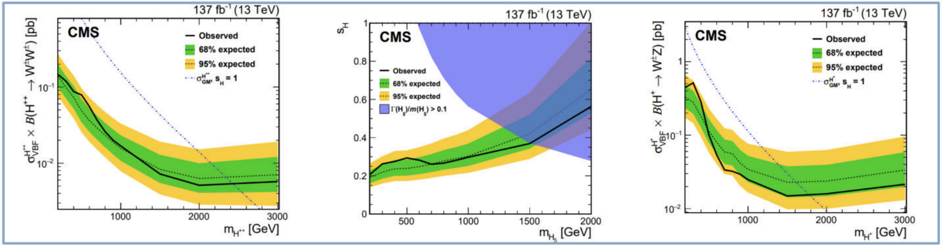

Simultaneous fits of $W_L W_L$ / $W_X W_T$ and $W_L W_X$ / $W_T W_T$ components in signal and control regions

- Polarization fraction of LL in the WW c.m. frame is the largest
- The interference between the polarized samples is expected to be small
- NLO α_S correction equal for all modes $\to$ applied to LL, TT, LT
- α_{EW} small for LL $\to$ applied to TT, uncertainty on LL LT

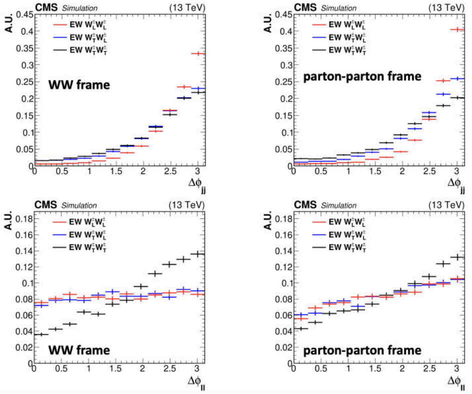

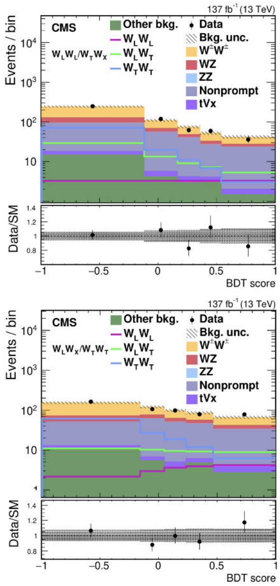

Two BDTs used to extract signal

- **Signal BDT**: trained to separate W_LW_L vs W_XW_T and W_LW_X vs W_TW_T. Different trainings for the WW and parton-parton c.m. frames with 15 discriminating variables
- **Inclusive BDT**: separate unpolarized EW $W^{\pm}W^{\pm}$ vs. non VBS events. Use 10 discriminating variables

Joint fit of 5 regions: SSWW-SR, WZ-SR, SSWW-CR, WZ-CR, ZZ-CR

2D distribution to extract signal: Signal BDT : Inclusive BDT

Leptonic $W^{\pm}W^{\pm} \rightarrow 2\ell 2\nu$ CMS

Source of uncertainty	$W^{\pm}_{L}W^{\pm}_{L}$ (%)	$W^{\pm}_{X}W^{\pm}_{T}$ (%)	$W^{\pm}_{L}W^{\pm}_{X}$ (%)	$W^{\pm}_{T}W^{\pm}_{T}$ (%)
Integrated luminosity	3.2	1.8	1.9	1.8
Lepton measurement	3.6	1.9	2.5	1.8
Jet energy scale and resolution	11	2.9	2.5	1.1
Pileup	0.9	0.1	1.0	0.3
b tagging	1.1	1.2	1.4	1.1
Nonprompt lepton rate	17	2.7	9.3	1.6
Trigger	1.9	1.1	1.6	0.9
Limited sample size	38	3.9	14	5.7
Theory	6.8	2.3	4.0	2.3
Total systematic uncertainty	44	6.6	18	7.0
Statistical uncertainty	123	15	42	22
Total uncertainty	130	16	46	23

Leptonic $W^\pm W^\pm \to 2\ell 2\nu$ CMS

The definition of fiducial region for the cross section measurements:

- Two same-sign leptons with $p_T > 20$ GeV, $|\eta| < 2.5$, $m_{\ell\ell} > 20$ GeV
- Two jets with $p_T > 20$ GeV, $|\eta| < 4.7$, $m_{jj} > 500$ GeV, $|\Delta\eta_{jj} > 2.5$

Measured fiducial cross sections for $W_L W_L$, $W_X W_T$, $W_L W_X$, and $W_T W_T$:
Good agreement with SM prediction*

Process	$\sigma\mathcal{B}$ (fb)	Theoretical prediction (fb)
$W^\pm_L W^\pm_L$	$0.32^{+0.42}_{-0.40}$	0.44 ± 0.05
$W^\pm_X W^\pm_T$	$3.06^{+0.51}_{-0.48}$	3.13 ± 0.35
$W^\pm_L W^\pm_X$	$1.20^{+0.56}_{-0.53}$	1.63 ± 0.18
$W^\pm_T W^\pm_T$	$2.11^{+0.49}_{-0.47}$	1.94 ± 0.21

WW c.m. frame

Process	$\sigma\mathcal{B}$ (fb)	Theoretical prediction (fb)
$W^\pm_L W^\pm_L$	$0.24^{+0.40}_{-0.37}$	0.28 ± 0.03
$W^\pm_X W^\pm_T$	$3.25^{+0.50}_{-0.48}$	3.32 ± 0.37
$W^\pm_L W^\pm_X$	$1.40^{+0.60}_{-0.57}$	1.71 ± 0.19
$W^\pm_T W^\pm_T$	$2.03^{+0.51}_{-0.50}$	1.89 ± 0.21

Parton-parton c.m. frame

The theoretical predictions including the $\alpha_S \alpha_{EW}^6$ and α^7 corrections to the MG5 LO cross section. The theoretical uncertainties include statistical, PDF, and LO scale uncertainties. $\mathcal{B}$ is the branching fraction for $WW \to \ell\ell\nu\nu$

Process	Yields in $W^{\pm}W^{\pm}$ SR
$W_L^{\pm}W_L^{\pm}$	16.0 ± 18.3
$W_L^{\pm}W_T^{\pm}$	63.1 ± 10.7
$W_T^{\pm}W_T^{\pm}$	110.1 ± 18.1
QCD $W^{\pm}W^{\pm}$	13.8 ± 1.6
Interference $W^{\pm}W^{\pm}$	8.4 ± 0.6
WZ	63.3 ± 7.8
ZZ	0.7 ± 0.2
Nonprompt	213.7 ± 52.3
tVx	7.1 ± 2.2
Other background	26.9 ± 9.9
Total SM	522.9 ± 60.7
Data	524

Leptonic $W^{\pm}W^{\pm} \to 2\ell 2\nu$ CMS

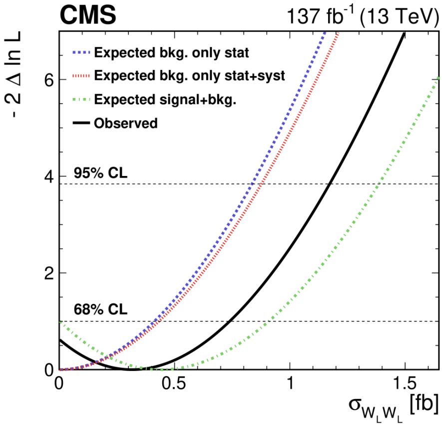

Profile likelihood ratio as a function of $W_L W_L$ cross section

- **WW c.m. frame**
  - σ Obs. (Exp.) = 2.3 (3.11) for $W_L W_X$
  - Observed (expected) limit of 1.17 (0.88) fb for $W_L W_L$ production
- **Parton-parton c.m. frame**
  - σ Obs. (Exp.) = 2.6 (2.9) for $W_L W_X$
  - Observed (expected) limit of 1.06 (0.85) fb for $W_L W_L$ production

Leptonic $W^{\pm}W^{\pm} \to \tau_h \ell 2\nu$ CMS

$W^{\pm}W^{\pm}$ VBS: minimum QCD-induced background. Exploit τ_h **channel for the first time in VBS**. Final state with 2 VBS-jets, high-pT e/μ τ_h and MET.

τ Decay	e	μ	π^-	$\pi^-\pi^0$	3π	Other
BR (%)	18	18	11	25	18	10

Backgrounds

- **Dominant Nonprompt** ($W + jets$, QCD) jets misidentified as leptons or τ_h, dedicated CR
- **Leptonic $t\bar{t}$**, normalization constrained in CR
- **Opposite sign** (VBS, Z/γ+jets), normalization constrained in CR

Region	EW-VBS	Fake	$t\bar{t}$	OS+Z/γ	QCD-VBS
SR $e\tau_h$	3.0%	92.2%	0.9%	2.0%	0.3%
SR $\mu\tau_h$	3.1%	93.3%	0.5%	1.7%	0.3%
$t\bar{t}$ CR	-	37.1%	61.6%	8.2%	-
OS CR	-	56.4%	7.9%	35.1%	-

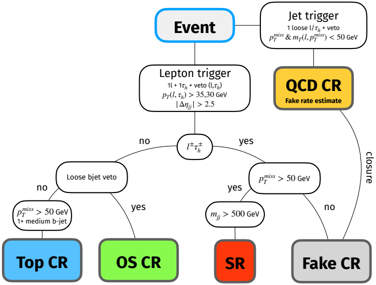

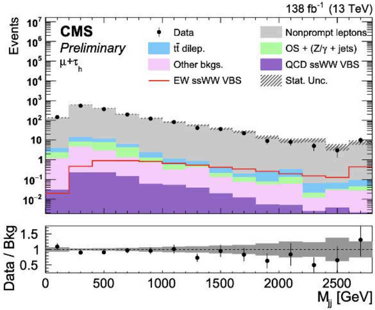

Leptonic $W^{\pm}W^{\pm} \to \tau_h \ell 2\nu$ CMS

Profiled likelihood fit to DNN spectra in SR and OS, Top CR → enhance discrimination of EW VBS from backgrounds:

- **SR + loose ℓ** (nonprompt proxy): W+jets, had/semilep $t\bar{t}$, Z/γ + jets
- **SR + tight ℓ**: ZZ, OS, leptonic $t\bar{t}$

EW $W^{\pm}W^{\pm}jj \to \ell\tau_h 2\nu jj$ significance of 2.7σ (2.9σ EW+QCD).

$$\mu_{EW} = 1.44^{+0.63}_{-0.53}; \quad \mu_{EW+QCD} = 1.43^{+0.60}_{-0.54}$$

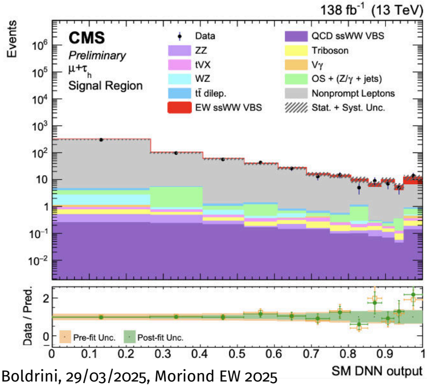

BSM search in the context of SMEFT up to dimension-8: no deviations from SM

Wilson coefficient		95% CL interval Observed	Expected
dim-6	c_W	$[-0.842, 0.818]$	$[-0.987, 0.974]$
	c_{HW}	$[-8.68, 7.60]$	$[-9.99, 9.05]$
dim-8	f_{T0}	$[-1.32, 1.38]$	$[-1.52, 1.58]$
	f_{M0}	$[-13.1, 12.8]$	$[-14.6, 14.5]$
	f_{S0}	$[-15.9, 16.1]$	$[-17.4, 17.9]$

$$|\mathcal{A}|^2 = |\mathcal{A}_{SM}|^2 + \sum_{\alpha} \frac{c_\alpha}{\Lambda^2} \cdot 2\,\mathrm{Re}(\mathcal{A}_{SM}\mathcal{A}^{\dagger}_{Q_\alpha}) + \sum_{\alpha,\beta} \frac{c_\alpha c_\beta}{\Lambda^4} \cdot (\mathcal{A}_{Q_\alpha}\mathcal{A}^{\dagger}_{Q_\beta})$$

$$+ \sum_i \left[\frac{f_i}{\Lambda^4} \cdot 2\,\mathrm{Re}(\mathcal{A}_{SM}\mathcal{A}^{\dagger}_{O_i}) + \frac{f_i^2}{\Lambda^8} \cdot |\mathcal{A}_{O_i}|^2 \right]$$

First time in VBS!

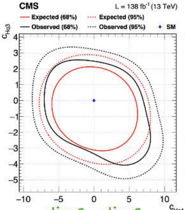

dim6 - dim6

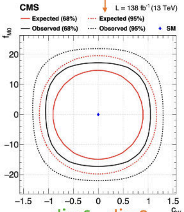

dim6 - dim8

Leptonic $W^+W^- \to 2l2\nu$ CMS

ATLAS: $e\mu 2\nu$, **CMS: $2l2\nu$** $\to$ different background composition with flavour

- *ee*, $\mu\mu$ additional DY contribution
- $e\mu$ DY reduced (low contamination from $\tau\tau \to e\mu$) $\to$ **Driving the sensitivity**

Fine regions definition based on Z_{ll} and $\Delta\eta_{jj}$.

Backgrounds

- **Dominant leptonic** $t\bar{t}$ and tW
- **DY** only in SF categories $\to$ divided into PU and no-PU
- **QCD-induced VBS**. No CR for this background but normalization freely floating
- **Nonprompt** mainly from W+jets, data driven estimate

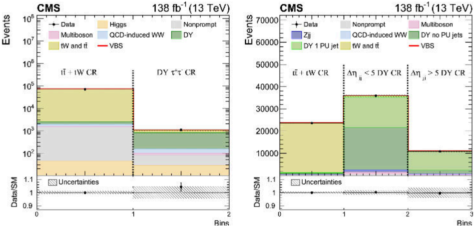

CR post-fit yeld. Right: $e\mu$, Left ee + $\mu\mu$

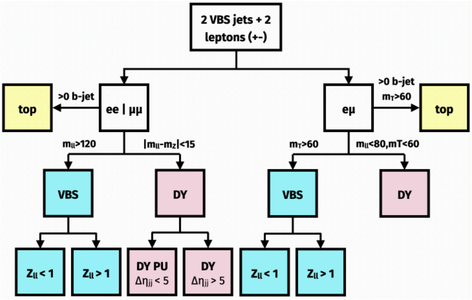

Leptonic $W^+W^- \to 2l2\nu$ CMS

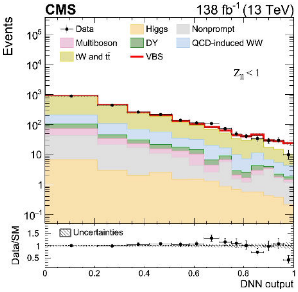

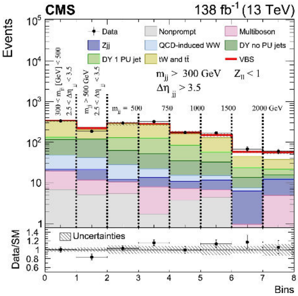

Lepton-flavour dependent signal extraction

Different flavour $e\mu$

- DNN trained against $t\bar{t}$, tW and QCD-VBS
- Different models for $Z_{ll} < 1$ and $Z_{ll} > 1$

Same flavour ee/$\mu\mu$

- 5 m_{jj} bins for $m_{jj} \geq 500$ GeV and $\Delta\eta \geq 3.5$
- 3 bins in $\Delta\eta$ and m_{jj} with lower sensitivity

The VBS EW production of $W^{\pm}W^{\mp}$ is observed with a significance 5.6σ (5.2 expected)

Two fiducial volumes (inclusive and exclusive) used to measure the process cross-section. **Good agreement with SM predictions at LO**

Fiducial region	σ measured	σ SM@LO
Inclusive	99 ± 20 fb	89 ± 5 fb
Exclusive	10.2 ± 2.0 fb	9.1 ± 0.6

Semi-leptonic VBS $W^{\pm}V \to l\nu jj$

First LHC evidence of a semileptonic VBS process. Final state with 4 jets, one charged lepton + MET. Search for WV VBS where the $W^{\pm} \to l^{\pm}\nu_l$ and $V(W^{\pm}/Z) \to q\bar{q}$

- **Resolved regime**: Four $R = 0.4$ jets resolved in ΔR
- **Boosted regime**: Two $R = 0.4$ and one $R = 0.8$ jets for boosted decays of the V-boson

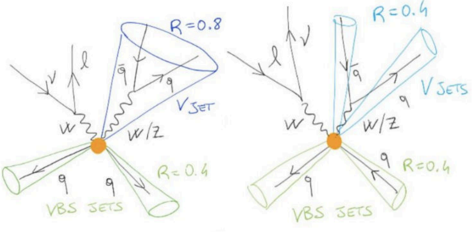

Harsh multijet background

- **Dominant W+jets** production → data driven based corrections in $p_T^{W,\ell}$ and $p_{T,j2}^{VBS}$ in CR.
- **semileptonic $t\bar{t}$ and single top**: constrained from data in b-enriched CR.
- **Non-prompt** mainly from QCD-multijet, data driven estimate

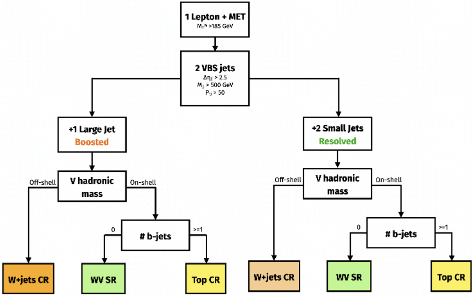

Semi-leptonic VBS $W^{\pm}V \rightarrow l\nu jj$

DNN is used for signal extraction (boost/res) which improves the significance of a factor 3 with respect to m_{jj} Results reported for **pure EW VBS** production, for the joint fit with the **QCD-induced background** and in **2 dimensions** for μ_{EW}, μ_{QCD}. **Measurement agrees with SM expectations**

Evidence for the VBS EW production of $W^{\pm}V \rightarrow l\nu jj$ with a significance of 4.4σ

$$\mu_{EW} = 0.85 \pm 0.12(\text{stat})^{+0.19}_{-0.17}(\text{syst}) = 0.85^{+0.23}_{-0.21}$$
$$\mu_{EW+QCD} = 0.97 \pm 0.06(\text{stat})^{+0.19}_{-0.21}(\text{syst}) = 0.97^{+0.20}_{-0.22}$$

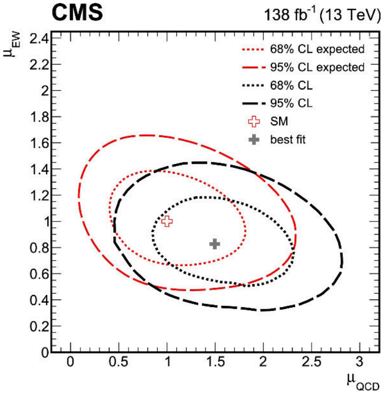

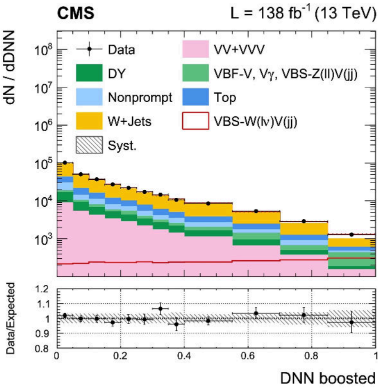

Semi-leptonic VBS $W^{\pm}V \to l\nu jj$

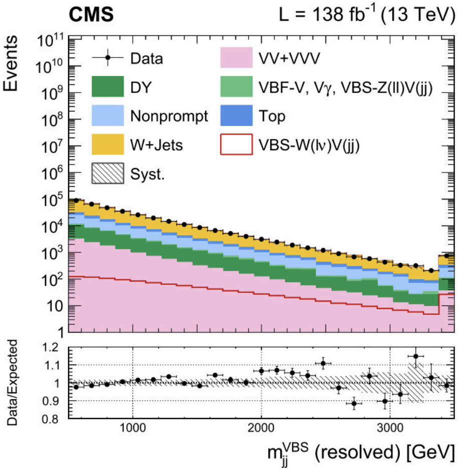

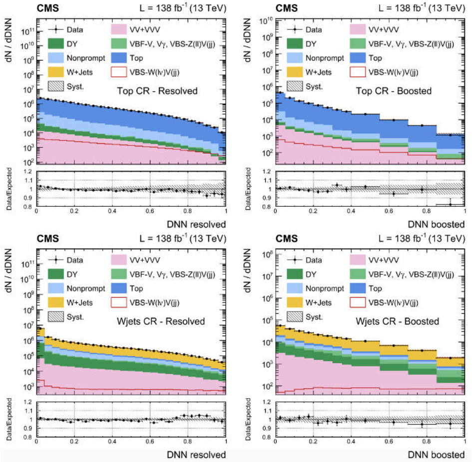

Semi-leptonic VBS $W^{\pm}V \to l\nu jj$

Table 2
Breakdown of the uncertainties in the EW WV VBS signal strength measurement.

Uncertainty source	$\Delta\mu_{EW}$
Statistical	0.12
Limited sample size	0.10
Normalization of backgrounds	0.08
Experimental	
b-tagging	0.05
Jet energy scale and resolution	0.04
Integrated luminosity	0.01
Lepton identification	0.01
Boosted V boson identification	0.01
Total	0.06
Theory	
Signal modeling	0.09
Background modeling	0.08
Total	0.12
Total	0.22

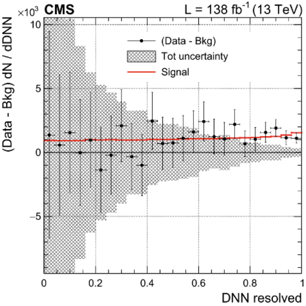

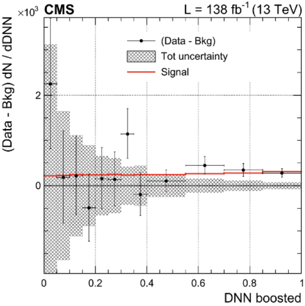

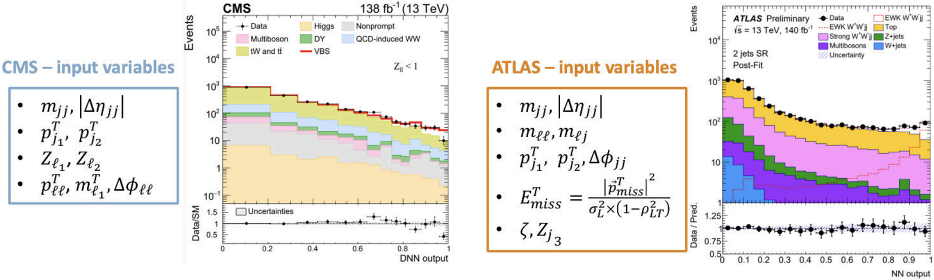

Figure: Slide from Mattia Lizzo

The most striking feature by ATLAS analysis is the $s/\sqrt{b}$ of the very last DNN bin, which ultimately is the key ingredient to reach the best possible sensitivity

- **CMS last bin**: $s \sim 14$, $b \sim 10 \to s/\sqrt{b} \sim 4.4$
- **ATLAS last bin**: $s \sim 60$, $b \sim 35 \to \boldsymbol{s/\sqrt{b} \sim 10.1}$

Leptonic $W^+W^- \to 2l2\nu$ CMS

Very different phase space definition from ATLAS and CMS in the $e\mu$ final state

- Same amount of signal between ATLAS and CMS driving region but less background in CMS
- ATLAS larger significance driven by discrimination power if the NN model (last bin)
- Signal (background) fraction in last bin: CMS $\sim$ 9%(0.4%), ATLAS $\sim$ 38%(0.6%)

	CMS signal region $(e\mu)$		ATLAS signal region	
	$Z_{\ell\ell} < 1$	$Z_{\ell\ell} > 1$	$n_{jet} = 2$	$n_{jet} = 3$
EWK W^+W^-jj	169 ± 20	70 ± 8	158 ± 27	54 ± 13
$t\bar{t} + tW$	1629 ± 71	1453 ± 70	2885 ± 214	1851 ± 131
QCD W^+W^-	327 ± 62	409 ± 77	1214 ± 256	514 ± 121
W + jets (fake)	107 ± 18	110 ± 16	37 ± 97	19 ± 48
Z + jets	69 ± 5	102 ± 6	216 ± 62	65 ± 25
Multiboson	68 ± 7	76 ± 7	101 ± 5	42 ± 3
Higgs	27 ± 2	20 ± 1	–	–
MC prediction	2397 ± 99	2240 ± 106	4610 ± 77	2546 ± 48
DATA	2441	2192	4610	2533

Figure: Slide from Mattia Lizzo

Input analyses

WV: DNN in boosted and resolved regions

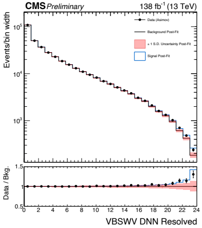

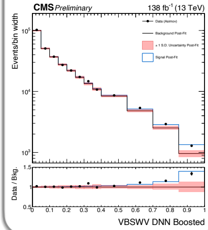

ZV: DNN in boosted and resolved regions

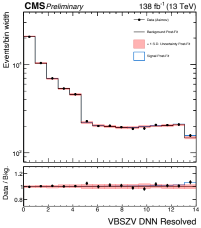

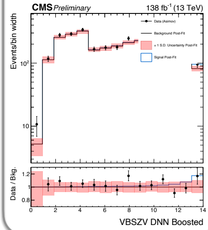

SSWW: mll:mjj WZ: BDT

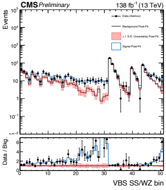

ZZ(4l): Matrix Element

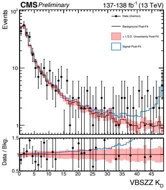

OSWW: DNN in high/low Zeppenfeld

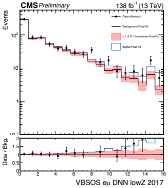

SSWW(τh): DNN

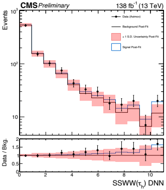

Observed input distributions in SRs after the combined fit.

Overlap 1/2

Table 14: Summary table of the signal regions defined in the analyses entering the combination along with some of the selections that make them orthogonal to each other

Region	n. ℓ	ℓ veto	SF	$\lvert\sum$ charge$\rvert$	b-veto	m_{ll}	MET	n. AK4
WV-SR	1	yes	-	1	yes	-	-	(≥ 4) or $(\geq 2 + \geq 1$ AK8)
SS-SR	2	yes	-	2	yes	> 20 GeV	> 30 GeV	≥ 2
OS-SR(SF)	2	yes	Yes	0	yes	> 120 GeV	> 60 GeV	≥ 2
OS-SR(DF)	2	yes	No	0	yes	> 50 GeV	> 20 GeV	≥ 2
ZV-SR(btag)	2	yes	Yes	0	no	$\in [76, 106]$ GeV	-	(≥ 4) or $(\geq 2 + \geq 1$ AK8)
ZV-SR(bveto)	2	yes	Yes	0	yes	$\in [76, 106]$ GeV	-	(≥ 4) or $(\geq 2 + \geq 1$ AK8)
WZ-SR	3	yes	Yes (Z)	1	yes	$\in [76, 106]$ GeV	> 30 GeV	≥ 2
ZZ-SR	4	yes	Yes	0	-	$\in [60, 120]$ GeV	-	≥ 2

Table 15: Summary table of the signal regions defined in the analyses entering the combination along with some of the selections that make them orthogonal to each other

Region	n. ℓ	ℓ veto	SF	$\lvert\sum$ charge$\rvert$	b-veto	m_{ll}	MET	n. AK4
SS-SR	2	yes	-	2	yes	> 20 GeV	> 30 GeV	≥ 2
OS-SR(SF)	2	yes	Yes	0	yes	> 120 GeV	> 60 GeV	≥ 2
OS-SR(DF)	2	yes	no	0	yes	> 50 GeV	> 20 GeV	≥ 2
ZV-Top	2	yes	no	0	-	$\in [76, 106]$ GeV	-	(≥ 4) or $(\geq 2 + \geq 1$ AK8)
OS-DY(DF)	2	yes	no	0	yes	$\in [50, 80]$ GeV	> 20 GeV	≥ 2
OS-DY(SF)	2	yes	yes	0	yes	$\in [76, 106]$ GeV	> 60 GeV	≥ 2
ZV-DY(bveto)	2	yes	yes	0	yes	$\in [76, 106]$ GeV	-	(≥ 4) or $(\geq 2 + \geq 1$ AK8)
ZV-SR(bveto)	2	yes	yes	0	yes	$\in [76, 106]$ GeV	-	(≥ 4) or $(\geq 2 + \geq 1$ AK8)

2 charged leptons regions: b-vetoed Negligible overlap

- SSWW SRs orthogonal to all other b-vetoed regions thanks to $|\sum \text{charge}| = \mathbf{2}$
- SSWW(τ_h) OS CR only region **requiring a τ_h**
- ZV Top CR partially overlap with OS-SR(DF), OS-DY(DF) $\rightarrow$ **Removed ZV Top CR**
- OSWW DY CR, ZV-DY and ZV-SR different MET requirements and target different kinematic regimes in number of jets: ZV SR $m_V \in [65, 105]$ inverted for ZV DY CR

Region	n. ℓ	ℓ/τ veto	SF	$\|\sum$ charge$\|$	b-veto	m_{ll}	MET	n. AK4
SS-SR	2	yes/yes	-	2	yes	> 20 GeV	> 30 GeV	≥ 2
SS(τ)-SR	2	yes/no	-	2	yes	-	> 50 GeV	≥ 2
SS(τ)-OS	2	yes/no	-	0	yes	-	-	≥ 2
OS-SR(SF)	2	yes/-	Yes	0	yes	> 120 GeV	> 60 GeV	≥ 2
OS-SR(DF)	2	yes/-	no	0	yes	> 50 GeV	> 20 GeV	≥ 2
OS-DY(DF)	2	yes/-	no	0	yes	$\in [50, 80]$ GeV	> 20 GeV	≥ 2
OS-DY(SF)	2	yes/-	yes	0	yes	$\in [76, 106]$ GeV	> 60 GeV	≥ 2
ZV-DY(bveto)	2	yes/-	yes	0	yes	$\in [76, 106]$ GeV	-	(≥ 4) or (≥ 2 + ≥ 1 AK8)
ZV-SR(bveto)	2	yes/-	yes	0	yes	$\in [76, 106]$ GeV	-	(≥ 4) or (≥ 2 + ≥ 1 AK8)

Potential overlaps from 2 charged leptons regions: b-tag

Negligible overlap

- SSWW-btag orthogonal to all other b-tag regions thanks to $|\sum \text{charge}| = \mathbf{2}$
- SSWW(τ_h) Top CR only region **requiring a τ_h**
- OSWW(ee, $\mu\mu$) Top CR orthogonal by SF requirements and $\boldsymbol{m_{\ell\ell}} > \mathbf{120}$ GeV
- ZV Top CR partially overlap with OS-SR(DF), OS-DY(DF) $\rightarrow$ **Removed ZV Top CR**
- ZV Top CR partially overlap with OS-Top CR ($e\mu$) $\rightarrow$ **Removed ZV Top CR**

Region	n. ℓ	ℓ/τ veto	SF	$\lvert\sum$ charge$\rvert$	b-veto	m_{ll}	MET	n. AK4
SS-b	2	yes/yes	-	2	no	$>$ 20 GeV	$>$ 30 GeV	$\geq$ 2
SS(τ)-Top	2	yes/no	-	0	no	-	$>$ 50 GeV	$\geq$ 2
OS-Top(SF)	2	yes/-	yes	0	no	$>$ 120 GeV	$>$ 60 GeV	$\geq$ 2
ZV-DY(btag)	2	yes/-	yes	0	no	$\in$ [76, 106] GeV	-	($\geq$ 4) or ($\geq$ 2 + $\geq$ 1 AK8)
ZV-SR(btag)	2	yes/-	yes	0	no	$\in$ [76, 106] GeV	-	($\geq$ 4) or ($\geq$ 2 + $\geq$ 1 AK8)
OS-Top(DF)	2	yes/-	no	0	no	$>$ 50 GeV	$>$ 20 GeV	$\geq$ 2

Other regions do not show significant overlaps

- WV CR only regions with 1 charged lepton and veto on additional ones
- SSWW/WZ ZZ CR not sensitive to EW $ZZ \to 4\ell$ but used to measure normalization of QCD-induced part $\to$ **Removed ZZ CR**

Region	n. ℓ	ℓ/τ veto	SF	$\lvert\sum$ charge$\rvert$	b-veto	m_{ll}	MET	n. AK4
WV-Top	1	yes/-	-	1	no	-	-	(≥ 4) or $(\geq 2 + \geq 1$ AK8)
WV-Wjets	1	yes/-	-	1	yes	-	-	(≥ 4) or $(\geq 2 + \geq 1$ AK8)
ZZ-SR	4	yes/-	yes	0	-	$\in [60, 120]$ GeV	-	≥ 2

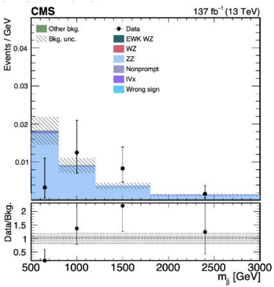

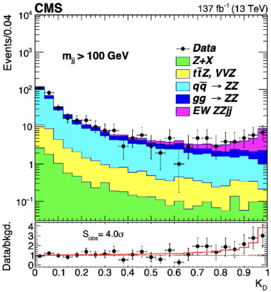

Table 16: Summary table of the signal regions defined in the analyses entering the combination along with some of the selections that make them orthogonal to each other

Region	n. ℓ	ℓ veto	SF	$\lvert\sum$ charge$\rvert$	b-veto	m_{ll}	MET	n. AK4
WV-Top	1	yes	-	1	no	-	-	(≥ 4) or $(\geq 2 + \geq 1$ AK8)
SS-b	2	yes	-	2	no	> 20 GeV	> 30 GeV	≥ 2
WZ-b	3	yes	yes (Z)	1	no	$\in [76, 106]$ GeV	> 30 GeV	≥ 2
OS-Top(SF)	2	yes	yes	0	no	> 120 GeV	> 60 GeV	≥ 2
ZV-DY(btag)	2	yes	yes	0	no	$\in [76, 106]$ GeV	-	(≥ 4) or $(\geq 2 + \geq 1$ AK8)
ZV-SR(btag)	2	yes	yes	0	no	$\in [76, 106]$ GeV	-	(≥ 4) or $(\geq 2 + \geq 1$ AK8)
ZV-Top	2	yes	no	0	-	$\in [76, 106]$ GeV	-	(≥ 4) or $(\geq 2 + \geq 1$ AK8)
OS-Top(DF)	2	yes	no	0	no	> 50 GeV	> 20 GeV	≥ 2

Table 17: Summary table of the signal regions defined in the analyses entering the combination along with some of the selections that make them orthogonal to each other

Region	n. ℓ	ℓ veto	SF	$\lvert\sum$ charge$\rvert$	b-veto	m_{ll}	MET	n. AK4
WV-Wjets	1	yes	-	1	yes	-	-	(≥ 4) or $(\geq 2 + \geq 1$ AK8)
ZZ-SR	4	yes	yes	0	-	$\in [60, 120]$ GeV	-	≥ 2
SS-ZZ	4	yes	yes	0	-	$\in [76, 106]$ GeV	-	≥ 2

Post-fit WV

Throw 500 toys from best post-fit value for each of the 4 POI and fit them to evaluate **post-fit background uncertainty**. * Signal is prefit (r=1) and data is Asimov

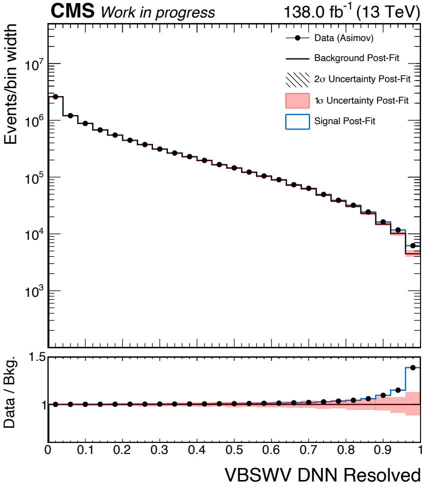

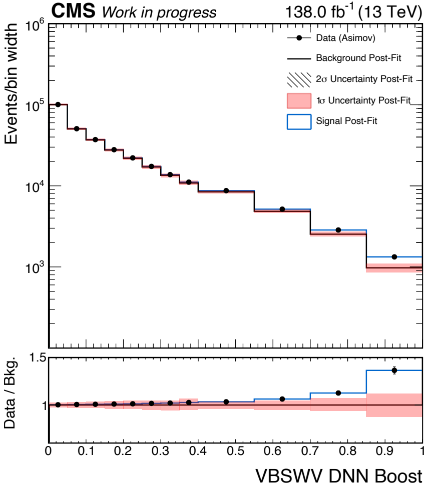

* Signal is prefit (r=1) and data is Asimov

Post-fit OSWW

Throw 500 toys from best post-fit value for each of the 4 POI and fit them to evaluate **post-fit background uncertainty**. * Signal is prefit (r=1) and data is Asimov

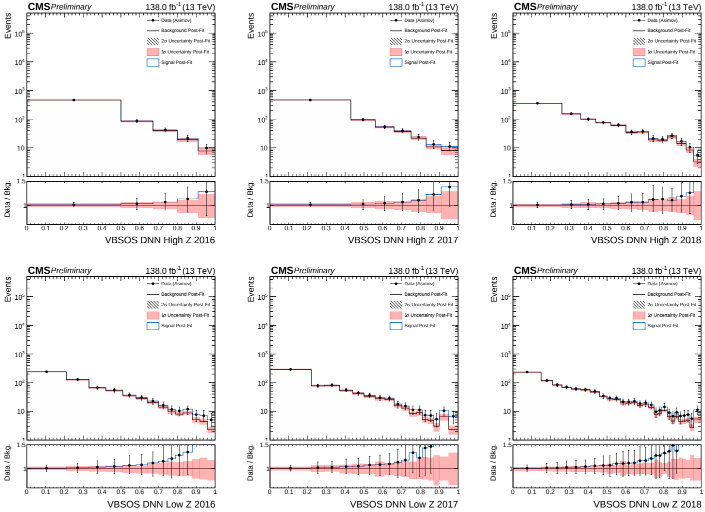

Post-fit

Throw 500 toys from best post-fit value for each of the 4 POI and fit them to evaluate **post-fit background uncertainty**. * Signal is prefit (r=1) and data is Asimov

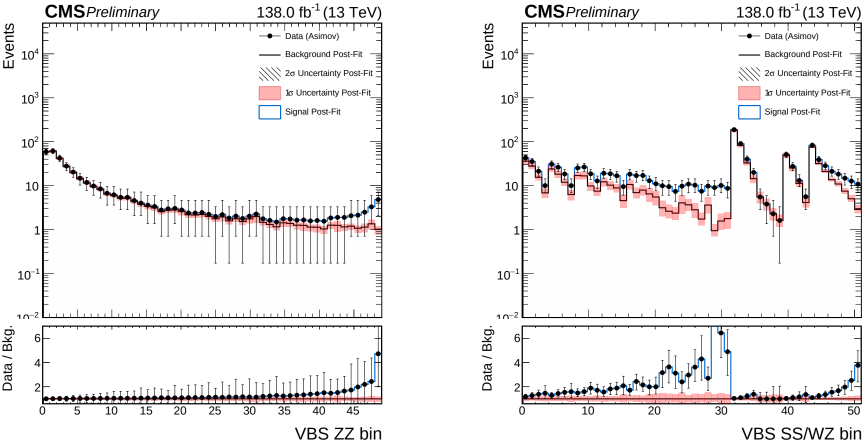

* Signal is prefit (r=1) and data is Asimov

Post-fit

Throw 500 toys from best post-fit value for each of the 4 POI and fit them to evaluate **post-fit background uncertainty**. * Signal is prefit (r=1) and data is Asimov

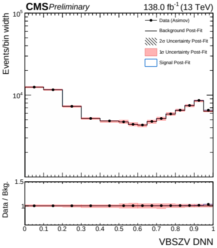

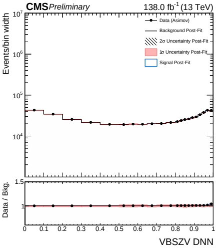

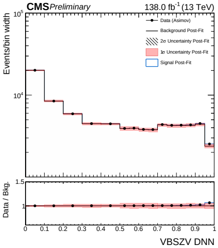

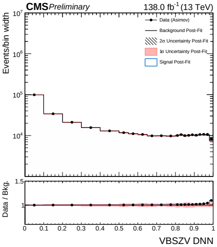

* Signal is prefit (r=1) and data is Asimov

Correlation tables

Nuisance	type	SS(e,μ)/WZ	SS(τ_h)	OSWW	WV	ZV	ZZ	Nuisance	type	SS(e,μ)/WZ	SS(τ_h)	OSWW	WV	ZV	ZZ
CMS_2e2mu_Zjets_2016	lnN	-	-	-	-	-	✓	CMS_2e2mu_Zjets_2017	lnN	-	-	-	-	-	✓
CMS_2e2mu_Zjets_2018	lnN	-	-	-	-	-	✓	CMS_4e_Zjets_2016	lnN	-	-	-	-	-	✓
CMS_4e_Zjets_2017	lnN	-	-	-	-	-	✓	CMS_4e_Zjets_2018	lnN	-	-	-	-	-	✓
CMS_4mu_Zjets_2016	lnN	-	-	-	-	-	✓	CMS_4mu_Zjets_2017	lnN	-	-	-	-	-	✓
CMS_4mu_Zjets_2018	lnN	-	-	-	-	-	✓	CMS_PS_FSR_DY	shape	-	-	-	✓	-	-
CMS_PS_FSR_QCD_WV	shape	-	-	-	✓	-	-	CMS_PS_FSR_QCD_ZV	shape	-	-	-	✓	-	-
CMS_PS_FSR_VBF-V_dipole	shape	-	-	-	✓	-	-	CMS_PS_FSR_VBS_WV	shape	-	-	-	✓	-	-
CMS_PS_FSR_VBS_ZV	shape	-	-	-	✓	-	-	CMS_PS_FSR_VVV	shape	-	-	-	✓	-	-
CMS_PS_FSR_Vg	shape	-	-	-	✓	-	-	CMS_PS_FSR_VgS	shape	-	-	-	✓	-	-
CMS_PS_FSR_Wjets_boost_1	shape	-	-	-	✓	-	-	CMS_PS_FSR_Wjets_boost_2	shape	-	-	-	✓	-	-
CMS_PS_FSR_Wjets_boost_3	shape	-	-	-	✓	-	-	CMS_PS_FSR_Wjets_boost_4	shape	-	-	-	✓	-	-
CMS_PS_FSR_Wjets_boost_5	shape	-	-	-	✓	-	-	CMS_PS_FSR_Wjets_boost_6	shape	-	-	-	✓	-	-
CMS_PS_FSR_Wjets_boost_7	shape	-	-	-	✓	-	-	CMS_PS_FSR_Wjets_res_1	shape	-	-	-	✓	-	-
CMS_PS_FSR_Wjets_res_10	shape	-	-	-	✓	-	-	CMS_PS_FSR_Wjets_res_11	shape	-	-	-	✓	-	-
CMS_PS_FSR_Wjets_res_12	shape	-	-	-	✓	-	-	CMS_PS_FSR_Wjets_res_13	shape	-	-	-	✓	-	-
CMS_PS_FSR_Wjets_res_14	shape	-	-	-	✓	-	-	CMS_PS_FSR_Wjets_res_15	shape	-	-	-	✓	-	-
CMS_PS_FSR_Wjets_res_16	shape	-	-	-	✓	-	-	CMS_PS_FSR_Wjets_res_17	shape	-	-	-	✓	-	-
CMS_PS_FSR_Wjets_res_18	shape	-	-	-	✓	-	-	CMS_PS_FSR_Wjets_res_19	shape	-	-	-	✓	-	-
CMS_PS_FSR_Wjets_res_2	shape	-	-	-	✓	-	-	CMS_PS_FSR_Wjets_res_20	shape	-	-	-	✓	-	-
CMS_PS_FSR_Wjets_res_21	shape	-	-	-	✓	-	-	CMS_PS_FSR_Wjets_res_3	shape	-	-	-	✓	-	-
CMS_PS_FSR_Wjets_res_4	shape	-	-	-	✓	-	-	CMS_PS_FSR_Wjets_res_5	shape	-	-	-	✓	-	-
CMS_PS_FSR_Wjets_res_6	shape	-	-	-	✓	-	-	CMS_PS_FSR_Wjets_res_7	shape	-	-	-	✓	-	-
CMS_PS_FSR_Wjets_res_8	shape	-	-	-	✓	-	-	CMS_PS_FSR_Wjets_res_9	shape	-	-	-	✓	-	-
CMS_PS_FSR_ggWW	shape	-	-	-	✓	-	-	CMS_PS_FSR_top	shape	-	-	-	✓	-	-
CMS_PS_ISR_DY	shape	-	-	-	✓	-	-	CMS_PS_ISR_QCD_WV	shape	-	-	-	✓	-	-
CMS_PS_ISR_QCD_ZV	shape	-	-	-	✓	-	-	CMS_PS_ISR_VBF-V_dipole	shape	-	-	-	✓	-	-
CMS_PS_ISR_VBS_WV	shape	-	-	-	✓	-	-	CMS_PS_ISR_VBS_ZV	shape	-	-	-	✓	-	-
CMS_PS_ISR_VVV	shape	-	-	-	✓	-	-	CMS_PS_ISR_Vg	shape	-	-	-	✓	-	-
CMS_PS_ISR_VgS	shape	-	-	-	✓	-	-	CMS_PS_ISR_Wjets_boost_1	shape	-	-	-	✓	-	-
CMS_PS_ISR_Wjets_boost_2	shape	-	-	-	✓	-	-	CMS_PS_ISR_Wjets_boost_3	shape	-	-	-	✓	-	-
CMS_PS_ISR_Wjets_boost_4	shape	-	-	-	✓	-	-	CMS_PS_ISR_Wjets_boost_5	shape	-	-	-	✓	-	-
CMS_PS_ISR_Wjets_boost_6	shape	-	-	-	✓	-	-	CMS_PS_ISR_Wjets_boost_7	shape	-	-	-	✓	-	-
CMS_PS_ISR_Wjets_res_1	shape	-	-	-	✓	-	-	CMS_PS_ISR_Wjets_res_10	shape	-	-	-	✓	-	-
CMS_PS_ISR_Wjets_res_11	shape	-	-	-	✓	-	-	CMS_PS_ISR_Wjets_res_12	shape	-	-	-	✓	-	-
CMS_PS_ISR_Wjets_res_13	shape	-	-	-	✓	-	-	CMS_PS_ISR_Wjets_res_14	shape	-	-	-	✓	-	-
CMS_PS_ISR_Wjets_res_15	shape	-	-	-	✓	-	-	CMS_PS_ISR_Wjets_res_16	shape	-	-	-	✓	-	-
CMS_PS_ISR_Wjets_res_17	shape	-	-	-	✓	-	-	CMS_PS_ISR_Wjets_res_18	shape	-	-	-	✓	-	-
CMS_PS_ISR_Wjets_res_19	shape	-	-	-	✓	-	-	CMS_PS_ISR_Wjets_res_2	shape	-	-	-	✓	-	-
CMS_PS_ISR_Wjets_res_20	shape	-	-	-	✓	-	-	CMS_PS_ISR_Wjets_res_21	shape	-	-	-	✓	-	-
CMS_PS_ISR_Wjets_res_3	shape	-	-	-	✓	-	-	CMS_PS_ISR_Wjets_res_4	shape	-	-	-	✓	-	-
CMS_PS_ISR_Wjets_res_5	shape	-	-	-	✓	-	-	CMS_PS_ISR_Wjets_res_6	shape	-	-	-	✓	-	-
CMS_PS_ISR_Wjets_res_7	shape	-	-	-	✓	-	-	CMS_PS_ISR_Wjets_res_8	shape	-	-	-	✓	-	-
CMS_PS_ISR_Wjets_res_9	shape	-	-	-	✓	-	-	CMS_PS_ISR_ggWW	shape	-	-	-	✓	-	-
CMS_PS_ISR_top	shape	-	-	-	✓	-	-	CMS_PU_2016	shape?	-	-	✓	✓	✓	-
CMS_PU_2017	shape	-	-	✓	✓	✓	-	CMS_PU_2018	shape?	-	-	✓	✓	✓	-
CMS_btag_cferr1	shape	-	-	✓	✓	✓	-	CMS_btag_cferr2	shape	-	-	✓	✓	✓	-
CMS_btag_heavy_2016	shape	✓	-	-	-	-	-	CMS_btag_heavy_2017	shape	✓	-	-	-	-	-
CMS_btag_heavy_2018	shape	✓	-	-	-	-	-	CMS_btag_hf	shape	-	-	✓	✓	✓	-
CMS_btag_hfstats1_2016	shape	-	-	✓	✓	✓	-	CMS_btag_hfstats1_2017	shape	-	-	✓	✓	✓	-
CMS_btag_hfstats1_2018	shape	-	-	✓	✓	✓	-	CMS_btag_hfstats2_2016	shape	-	-	✓	✓	✓	-
CMS_btag_hfstats2_2017	shape	-	-	✓	✓	✓	-	CMS_btag_hfstats2_2018	shape	-	-	✓	✓	✓	-
CMS_btag_jes	shape	-	-	✓	✓	✓	-	CMS_btag_lf	shape	-	-	✓	✓	✓	-
CMS_btag_lfstats1_2016	shape	-	-	✓	✓	✓	-	CMS_btag_lfstats1_2017	shape	-	-	✓	✓	✓	-
CMS_btag_lfstats1_2018	shape	-	-	✓	✓	✓	-	CMS_btag_lfstats2_2016	shape	-	-	✓	✓	✓	-
CMS_btag_lfstats2_2017	shape	-	-	✓	✓	✓	-	CMS_btag_lfstats2_2018	shape	-	-	✓	✓	✓	-
CMS_btag_light_2016	shape	✓	-	-	-	-	-	CMS_btag_light_2017	shape	✓	-	-	-	-	-
CMS_btag_light_2018	shape	✓	-	-	-	-	-	CMS_eff_e	shape	✓	-	-	-	-	-
CMS_eff_e_2016	shape	-	-	✓	✓	✓	✓	CMS_eff_e_2017	shape?	-	-	✓	✓	✓	✓
CMS_eff_e_2018	shape	-	-	✓	✓	✓	✓	CMS_eff_m	shape	✓	-	-	-	-	-
CMS_eff_m_2016	shape	-	-	✓	✓	✓	✓	CMS_eff_m_2017	shape?	-	-	✓	✓	✓	✓
CMS_eff_m_2018	shape	-	-	✓	✓	✓	✓	CMS_eff_prefiring_2016	shape?	✓	-	✓	✓	✓	✓
CMS_eff_prefiring_2016_ewk_ZZ	shape	-	-	-	-	-	✓	CMS_eff_prefiring_2017	shape?	✓	-	✓	✓	✓	✓
CMS_eff_prefiring_2017_ewk_ZZ	shape	-	-	-	-	-	✓	CMS_eff_prefiring_2018	shape	✓	-	-	-	-	-
CMS_eff_trigger_2016	shape	-	-	✓	✓	✓	-	CMS_eff_trigger_2017	shape	-	-	✓	✓	✓	-
CMS_eff_trigger_2018	shape	-	-	✓	✓	✓	-	CMS_embed_veto_2016	lnN	-	-	✓	-	-	-
CMS_embed_veto_2017	lnN	-	-	✓	-	-	-	CMS_embed_veto_2018	lnN	-	-	✓	-	-	-
CMS_fakeE3L_2016	shape	✓	-	-	-	-	-	CMS_fakeE3L_2017	shape	✓	-	-	-	-	-
CMS_fakeE3L_2018	shape	✓	-	-	-	-	-	CMS_fakeE_2016	shape	✓	-	-	-	-	-
CMS_fakeE_2017	shape	✓	-	-	-	-	-	CMS_fakeE_2018	shape	✓	-	-	-	-	-
CMS_fakeM3L_2016	shape	✓	-	-	-	-	-	CMS_fakeM3L_2017	shape	✓	-	-	-	-	-
CMS_fakeM3L_2018	shape	✓	-	-	-	-	-	CMS_fakeM_2016	shape	✓	-	-	-	-	-
CMS_fakeM_2017	shape	✓	-	-	-	-	-	CMS_fakeM_2018	shape	✓	-	-	-	-	-
CMS_fake_e_2016	shape	-	-	✓	✓	✓	-	CMS_fake_e_2017	shape	-	-	✓	✓	✓	-
CMS_fake_e_2018	shape	-	-	✓	✓	✓	-	CMS_fake_m_2016	shape	-	-	✓	✓	✓	-
CMS_fake_m_2017	shape	-	-	✓	✓	✓	-	CMS_fake_m_2018	shape	-	-	✓	✓	✓	-
CMS_fake_stat_e_2016	shape	-	-	✓	✓	✓	-	CMS_fake_stat_e_2017	shape	-	-	✓	✓	✓	-
CMS_fake_stat_e_2018	shape	-	-	✓	✓	✓	-	CMS_fake_stat_m_2016	shape	-	-	✓	✓	✓	-
CMS_fake_stat_m_2017	shape	-	-	✓	✓	✓	-	CMS_fake_stat_m_2018	shape	-	-	✓	✓	✓	-
CMS_fake_syst	lnN	-	-	-	-	✓	-	CMS_fake_syst_e	lnN	-	-	✓	-	-	-
CMS_fake_syst_e_WV	lnN	-	-	-	✓	-	-	CMS_fake_syst_em	lnN	-	-	-	-	✓	-
CMS_fake_syst_m	lnN	-	-	✓	-	-	-	CMS_fake_syst_m_WV	lnN	-	-	-	✓	-	-
CMS_fatjet_jmr_2016	shape	-	-	-	✓	✓	-	CMS_fatjet_jmr_2017	shape?	-	-	-	✓	✓	-
CMS_fatjet_jmr_2018	shape	-	-	-	✓	✓	-	CMS_fatjet_jms_2016	shape?	-	-	-	✓	✓	-
CMS_fatjet_jms_2017	shape	-	-	-	✓	✓	-	CMS_fatjet_jms_2018	shape?	-	-	-	✓	✓	-
CMS_fatjet_res_2017	lnN	-	-	-	✓	-	-	CMS_fatjet_res_2018	shape?	-	-	-	✓	✓	-
CMS_fatjet_tau21eff_2016	shape	-	-	-	✓	-	-	CMS_fatjet_tau21eff_2017	shape	-	-	-	✓	-	-
CMS_fatjet_tau21eff_2018	shape	-	-	-	✓	-	-	CMS_fj_scale_JESAbsolute	lnN	-	-	-	✓	-	-
CMS_fj_scale_JESAbsolute_2016	lnN	-	-	-	✓	-	-	CMS_fj_scale_JESAbsolute_2017	lnN	-	-	-	✓	-	-
CMS_fj_scale_JESAbsolute_2018	lnN	-	-	-	✓	-	-	CMS_fj_scale_JESBBEC1	lnN	-	-	-	✓	-	-
CMS_fj_scale_JESBBEC1_2016	lnN	-	-	-	✓	-	-	CMS_fj_scale_JESBBEC1_2017	lnN	-	-	-	✓	-	-
CMS_fj_scale_JESBBEC1_2018	lnN	-	-	-	✓	-	-	CMS_fj_scale_JESEC2	lnN	-	-	-	✓	-	-
CMS_fj_scale_JESEC2_2016	lnN	-	-	-	✓	-	-	CMS_fj_scale_JESEC2_2017	lnN	-	-	-	✓	-	-
CMS_fj_scale_JESEC2_2018	lnN	-	-	-	✓	-	-	CMS_fj_scale_JESFlavorQCD	lnN	-	-	-	✓	-	-
CMS_fj_scale_JESHF	lnN	-	-	-	✓	-	-	CMS_fj_scale_JESHF_2016	lnN	-	-	-	✓	-	-
CMS_fj_scale_JESHF_2017	lnN	-	-	-	✓	-	-	CMS_fj_scale_JESHF_2018	lnN	-	-	-	✓	-	-
CMS_fj_scale_JESRelativeBal	lnN	-	-	-	✓	-	-	CMS_fj_scale_JESRelativeSample_2016	lnN	-	-	-	✓	-	-
CMS_fj_scale_JESRelativeSample_2017	lnN	-	-	-	✓	-	-	CMS_fj_scale_JESRelativeSample_2018	lnN	-	-	-	✓	-	-
CMS_fj_tau21ptextr_2016	shape	-	-	-	✓	-	-	CMS_fj_tau21ptextr_2017	shape	-	-	-	✓	-	-
CMS_fj_tau21ptextr_2018	shape	-	-	-	✓	-	-	CMS_hww_CRSR_accept_DY	lnN	-	-	✓	-	-	-
CMS_hww_CRSR_accept_top	lnN	-	-	✓	-	-	-	CMS_hww_VZScale	lnN	-	-	✓	-	-	-
CMS_hww_VgStarScale	lnN	-	-	✓	-	-	-	CMS_jetpuid_2016	shape	-	-	✓	✓	✓	-
CMS_jetpuid_2017	shape	-	-	✓	✓	✓	-	CMS_jetpuid_2018	shape	-	-	✓	✓	✓	-
CMS_pu	shape	✓	-	-	-	-	-	CMS_res_j_2016	shape?	✓	-	-	-	-	✓
CMS_res_j_2017	shape	✓	-	✓	✓	✓	✓	CMS_res_j_2018	shape?	✓	-	✓	✓	✓	✓
CMS_scale_JESAbsolute	shape	-	-	✓	✓	✓	-	CMS_scale_JESAbsolute_2016	shape?	-	-	✓	✓	✓	-
CMS_scale_JESAbsolute_2017	shape	-	-	✓	✓	✓	-	CMS_scale_JESAbsolute_2018	shape?	-	-	✓	✓	✓	-
CMS_scale_JESBBEC1	shape	-	-	✓	✓	✓	-	CMS_scale_JESBBEC1_2016	shape?	-	-	✓	✓	✓	-
CMS_scale_JESBBEC1_2017	shape	-	-	✓	✓	✓	-	CMS_scale_JESBBEC1_2018	shape?	-	-	✓	✓	✓	-
CMS_scale_JESEC2	shape	-	-	✓	✓	✓	-	CMS_scale_JESEC2_2016	shape?	-	-	✓	✓	✓	-
CMS_scale_JESEC2_2017	shape	-	-	✓	✓	✓	-	CMS_scale_JESEC2_2018	shape?	-	-	✓	✓	✓	-

Nuisance	type	SS(e,μ)/WZ	SS(τ_h)	OSWW	WV	ZV	ZZ
CMS_scale_JESFlavorQCD	shape	-	-	✓	✓	✓	-
CMS_scale_JESHF_2016	shape	-	-	✓	✓	✓	-
CMS_scale_JESHF_2018	shape	-	-	✓	✓	✓	-
CMS_scale_JESRelativeSample_2016	shape	-	-	✓	✓	✓	-
CMS_scale_JESRelativeSample_2018	shape	-	-	✓	✓	✓	-
CMS_scale_cleanfatJER_2017	shape	-	-	-	-	✓	-
CMS_scale_cleanfatJES_2016	shape	-	-	-	-	✓	-
CMS_scale_cleanfatJES_2018	shape	-	-	-	-	✓	-
CMS_scale_e_2016	shape	-	-	✓	✓	✓	-
CMS_scale_e_2018	shape	-	-	✓	✓	✓	-
CMS_scale_j_2017	shape	✓	-	-	-	-	✓
CMS_scale_m	lnN	✓	-	-	-	-	-
CMS_scale_mVjer_2017	shape	-	-	-	-	✓	-
CMS_scale_mVjesTotal_2017	shape	-	-	-	-	✓	-
CMS_scale_m_2016	shape	-	-	✓	✓	✓	-
CMS_scale_m_2018	shape	-	-	✓	✓	✓	-
CMS_scale_met_2017	lnN	-	-	✓	✓	-	-
CMS_topPtRew	shape	-	-	-	✓	✓	-
CMS_trigger_2017	shape	✓	-	-	-	-	-
CMS_wseff	shape	✓	-	-	-	-	-
EWKqqZZCorr	shape	✓	-	-	-	-	-
FR_sys_electron_2016M	lnN	-	✓	-	-	-	-
FR_sys_electron_2018	lnN	-	✓	-	-	-	-
FR_sys_muon_2017	lnN	-	✓	-	-	-	-
FSR	shape	-	✓	-	-	-	-
PF	shape	-	✓	-	-	-	-
PS_ISR	shape	-	-	✓	-	✓	✓
QCDScale_TVX	shape	-	✓	-	-	-	-
QCDScale_VG	shape	-	✓	-	-	-	-
QCDScale_WpWpJJ_QCD	shape	-	✓	-	-	-	-
QCDScale_ZZtoLep	shape	-	✓	-	-	-	-
QCDScale_sig	shape	-	✓	-	-	-	-
QCDscale_DY	shape	-	-	✓	✓	✓	-
QCDscale_IntfWZ_ACCEPT	shape	✓	-	-	-	-	-
QCDscale_QCD_OSWW	shape	-	-	✓	✓	-	-
QCDscale_QCD_WZ	shape	-	-	-	✓	-	-
QCDscale_TVX	shape	✓	-	-	-	✓	-
QCDscale_VBS_VV_QCD	shape	-	-	-	-	✓	-
QCDscale_VH	lnN	-	-	✓	-	-	-
QCDscale_VVV	shape	-	-	-	✓	✓	-
QCDscale_Vg	shape	-	-	-	✓	✓	-
QCDscale_WJets	shape	-	-	-	✓	✓	-
QCDscale_WWewk_AsLnN	lnN	-	-	✓	-	-	-
QCDscale_ZZ_ACCEPT	shape	✓	-	-	-	-	-
QCDscale_ewk_SSWW	shape	✓	-	-	✓	-	-
QCDscale_ewk_ZZ	shape	-	-	-	✓	-	✓
QCDscale_ggZH	lnN	-	-	✓	-	-	-
QCDscale_qcd_ZZ	shape	-	-	-	-	-	✓
QCDscale_qqbar_ACCEPT	lnN	-	-	✓	-	-	-
QCDscale_ttH	lnN	-	-	✓	-	-	-
QGLmorph_gluon_higheta_16	shape	-	-	-	✓	-	-
QGLmorph_gluon_loweta_16	shape	-	-	-	✓	-	-
QGLmorph_quark_higheta_16	shape	-	-	-	✓	-	-
QGLmorph_quark_loweta_16	shape	-	-	-	✓	-	-
TES	shape	-	✓	-	-	-	-
THU_ggH_Mig12	shape	-	-	✓	-	-	-
THU_ggH_PT120	shape	-	-	✓	-	-	-
THU_ggH_Res	shape	-	-	✓	-	-	-
THU_ggH_VBF3j	shape	-	-	✓	-	-	-
THU_qqH_EWK	shape	-	-	✓	-	-	-
THU_qqH_Mjj1000	shape	-	-	✓	-	-	-
THU_qqH_Mjj1500	shape	-	-	✓	-	-	-
THU_qqH_Mjj60	shape	-	-	✓	-	-	-
THU_qqH_PTH200	shape	-	-	✓	-	-	-
THU_qqH_YIELD	shape	-	-	✓	-	-	-
UE_CUET	lnN	-	-	✓	✓	✓	-
VBS_2017	shape	-	✓	-	-	-	-
WZTauH	shape	✓	-	-	-	-	-
btag	shape	-	✓	-	-	-	-
jer_2016M	shape	-	✓	-	-	-	-
jer_2018	shape	-	✓	-	-	-	-
jes_TTTo2L2Nu_2017	lnN	-	✓	-	-	-	-
jes_TVX_2016M	lnN	-	✓	-	-	-	-
jes_TVX_2018	lnN	-	✓	-	-	-	-
jes_Triboson_2017	lnN	-	✓	-	-	-	-
jes_VG_2016M	lnN	-	✓	-	-	-	-
jes_VG_2018	lnN	-	✓	-	-	-	-
jes_WZ_2017	lnN	-	✓	-	-	-	-
jes_WpWpJJ_QCD_2016M	lnN	-	✓	-	-	-	-
jes_WpWpJJ_QCD_2018	lnN	-	✓	-	-	-	-
jes_WrongSign_2017	lnN	-	✓	-	-	-	-
jes_ZZtoLep_2016M	lnN	-	✓	-	-	-	-
jes_ZZtoLep_2018	lnN	-	✓	-	-	-	-
jes_sig_2017	lnN	-	✓	-	-	-	-
lep_2016M	shape	-	✓	-	-	-	-
lep_2018	shape	-	✓	-	-	-	-
lumi_13TeV_2017	lnN	✓	-	✓	✓	✓	✓
lumi_13TeV_BBDefl	lnN	✓	-	✓	✓	✓	✓
lumi_13TeV_DynBeta	lnN	-	-	-	✓	✓	-
lumi_13TeV_LSCale	lnN	✓	-	✓	✓	✓	✓
lumi_161718	lnN	-	✓	-	-	-	-
lumi_2016M	lnN	-	✓	-	-	-	-
lumi_2018	lnN	-	✓	-	-	-	-
mischarge_electron_2016M	lnN	-	✓	-	-	-	-
mischarge_electron_2018	lnN	-	✓	-	-	-	-
mischarge_muon_2017	lnN	-	✓	-	-	-	-
mistag	shape	-	✓	-	-	-	-
pdf_Higgs_gg	lnN	-	-	✓	-	-	-
pdf_Higgs_qqbar	lnN	-	-	✓	-	-	-
pdf_Higgs_ttH	lnN	-	-	✓	-	-	-
pdf_ewk_ZZ_16	lnN	-	-	-	-	-	✓
pdf_ewk_ZZ_1718bar	lnN	-	-	-	-	-	✓
pdf_qcd_16	lnN	-	-	-	-	-	✓
pdf_qcdloop_1718	lnN	-	-	-	-	-	✓
pdf_qqbar_ACCEPT	lnN	-	-	✓	-	-	-
puID	shape	-	✓	-	-	-	-
tau_vsele_2016M	shape	-	✓	-	-	-	-
tau_vsele_2018	shape	-	✓	-	-	-	-
tau_vsjet_2017	shape	-	✓	-	-	-	-
tau_vsmu_2016M	shape	-	✓	-	-	-	-

Nuisance	type	SS(e,μ)/WZ	SS(τ_h)	OSWW	WV	ZV	ZZ
CMS_scale_JESHF	shape?	-	-	✓	✓	✓	-
CMS_scale_JESHF_2017	shape?	-	-	✓	✓	✓	-
CMS_scale_JESRelativeBal	shape?	-	-	✓	✓	✓	-
CMS_scale_JESRelativeSample_2017	shape?	-	-	✓	✓	✓	-
CMS_scale_cleanfatJER_2016	shape	-	-	-	-	✓	-
CMS_scale_cleanfatJER_2018	shape	-	-	-	-	✓	-
CMS_scale_cleanfatJES_2017	shape	-	-	-	-	✓	-
CMS_scale_e	lnN	✓	-	-	-	-	-
CMS_scale_e_2017	shape?	-	-	✓	✓	✓	-
CMS_scale_j_2016	shape	✓	-	-	-	-	✓
CMS_scale_j_2018	shape	✓	-	-	-	-	✓
CMS_scale_mVjer_2016	shape	-	-	-	-	✓	-
CMS_scale_mVjesTotal_2016	shape	-	-	-	-	✓	-
CMS_scale_mVjesTotal_2018	shape	-	-	-	-	✓	-
CMS_scale_m_2017	shape?	-	-	✓	✓	✓	-
CMS_scale_met_2016	lnN	-	-	✓	✓	-	-
CMS_scale_met_2018	lnN	-	-	✓	✓	-	-
CMS_trigger_2016	shape	✓	-	-	-	-	-
CMS_trigger_2018	shape	✓	-	-	-	-	-
EWKCorrVVWZ	shape	✓	-	-	-	-	-
FES	shape	-	✓	-	-	-	-
FR_sys_electron_2017	lnN	-	✓	-	-	-	-
FR_sys_muon_2016M	lnN	-	✓	-	-	-	-
FR_sys_muon_2018	lnN	-	✓	-	-	-	-
ISR	shape	-	✓	-	-	-	-
PS_FSR	shape?	-	-	✓	-	✓	-
QCDScale_TTTo2L2Nu	shape	-	✓	-	-	-	-
QCDScale_Triboson	shape	-	✓	-	-	-	-
QCDScale_WZ	shape	-	✓	-	-	-	-
QCDScale_WrongSign	shape	-	✓	-	-	-	-
QCDScale_qcdloop_ZZ	lnN	-	-	-	-	-	✓
QCDscale_AsLnN	lnN	-	-	✓	-	-	-
QCDscale_IntfWW_ACCEPT	shape	✓	-	-	-	-	-
QCDscale_Other_ACCEPT	shape	✓	-	-	-	-	-
QCDscale_QCD_SSWW	shape	✓	-	-	✓	-	-
QCDscale_QCD_ZZ	shape	-	-	-	✓	-	-
QCDscale_VBF-V	shape	-	-	-	✓	✓	-
QCDscale_VG_ACCEPT	shape	✓	-	-	-	-	-
QCDscale_VV	shape	-	-	✓	-	-	-
QCDscale_VZ	shape	-	-	-	-	✓	-
QCDscale_VgS	shape	-	-	-	✓	✓	-
QCDscale_WS_ACCEPT	shape	✓	-	-	-	-	-
QCDscale_WZ_ACCEPT	shape	✓	-	-	-	-	-
QCDscale_ewk_OSWW	shape	-	-	✓	✓	-	-
QCDscale_ewk_WZ	shape	✓	-	-	✓	-	-
QCDscale_ggVV	lnN	-	-	✓	-	-	-
QCDscale_gg_ACCEPT	lnN	-	-	✓	-	-	-
QCDscale_qqH	lnN	-	-	✓	-	-	-
QCDscale_top	shape	-	-	✓	✓	✓	-
QCDscale_ttZ_tribos	lnN	-	-	-	-	-	✓
QGLmorph_gluon_higheta_1718	shape	-	-	-	✓	-	-
QGLmorph_gluon_loweta_1718	shape	-	-	-	✓	-	-
QGLmorph_quark_higheta_1718	shape	-	-	-	✓	-	-
QGLmorph_quark_loweta_1718	shape	-	-	-	✓	-	-
THU_ggH_Mig01	shape	-	-	✓	-	-	-
THU_ggH_Mu	shape	-	-	✓	-	-	-
THU_ggH_PT60	shape	-	-	✓	-	-	-
THU_ggH_VBF2j	shape	-	-	✓	-	-	-
THU_ggH_qmtop	shape	-	-	✓	-	-	-
THU_qqH_JET01	shape	-	-	✓	-	-	-
THU_qqH_Mjj120	shape	-	-	✓	-	-	-
THU_qqH_Mjj350	shape	-	-	✓	-	-	-
THU_qqH_Mjj700	shape	-	-	✓	-	-	-
THU_qqH_PTH25	shape	-	-	✓	-	-	-
UE_CP5	lnN	-	-	✓	✓	✓	-
VBS_2016M	shape	-	✓	-	-	-	-
VBS_2018	shape	-	✓	-	-	-	-
WZTauL	shape	✓	-	-	-	-	-
ggZZCorr	shape	✓	-	-	-	-	-
jer_2017	shape	-	✓	-	-	-	-
jes_TTTo2L2Nu_2016M	lnN	-	✓	-	-	-	-
jes_TTTo2L2Nu_2018	lnN	-	✓	-	-	-	-
jes_TVX_2017	lnN	-	✓	-	-	-	-
jes_Triboson_2016M	lnN	-	✓	-	-	-	-
jes_Triboson_2018	lnN	-	✓	-	-	-	-
jes_VG_2017	lnN	-	✓	-	-	-	-
jes_WZ_2016M	lnN	-	✓	-	-	-	-
jes_WZ_2018	lnN	-	✓	-	-	-	-
jes_WpWpJJ_QCD_2017	lnN	-	✓	-	-	-	-
jes_WrongSign_2016M	lnN	-	✓	-	-	-	-
jes_WrongSign_2018	lnN	-	✓	-	-	-	-
jes_ZZtoLep_2017	lnN	-	✓	-	-	-	-
jes_sig_2016M	lnN	-	✓	-	-	-	-
jes_sig_2018	lnN	-	✓	-	-	-	-
lep_2017	shape	-	✓	-	-	-	-
lumi_13TeV_2016	lnN	✓	-	✓	✓	✓	✓
lumi_13TeV_2018	lnN	✓	-	✓	✓	✓	✓
lumi_13TeV_CurrCalib	lnN	✓	-	✓	✓	✓	✓
lumi_13TeV_Ghosts	lnN	✓	-	✓	✓	✓	✓
lumi_13TeV_XYFact	lnN	✓	-	✓	✓	✓	✓
lumi_1718	lnN	-	✓	-	-	-	-
lumi_2017	lnN	-	✓	-	-	-	-
metUnclust	shape	-	✓	-	-	-	-
mischarge_electron_2017	lnN	-	✓	-	-	-	-
mischarge_muon_2016M	lnN	-	✓	-	-	-	-
mischarge_muon_2018	lnN	-	✓	-	-	-	-
pdf_1718	shape?	-	-	-	✓	✓	-
pdf_Higgs_gg_ACCEPT	lnN	-	-	✓	-	-	-
pdf_Higgs_qqbar_ACCEPT	lnN	-	-	✓	-	-	-
pdf_Tot	shape	-	✓	-	-	-	-
pdf_ewk_ZZ_1718	lnN	-	-	-	-	-	✓
pdf_gg_ACCEPT	lnN	-	-	✓	-	-	-
pdf_qcdloop_16	lnN	-	-	-	-	-	✓
pdf_qqbar	shape?	✓	-	✓	-	-	-
pu	shape	-	✓	-	-	-	-
singleTopToTTbar	shape	-	-	✓	✓	-	-
tau_vsele_2017	shape	-	✓	-	-	-	-
tau_vsjet_2016M	shape	-	✓	-	-	-	-
tau_vsjet_2018	shape	-	✓	-	-	-	-
tau_vsmu_2017	shape	-	✓	-	-	-	-

Simultaneous scan of signal strength pairs. Other μ profiled with nuisance parameters. Only mild correlations observed. Good agreement with SM expectations